



National Technical University of Athens

Department of Chemical Engineering

Section of Analysis, Design, and Development of Processes and Systems

Chemical Process Engineering Laboratory

Diploma Thesis

# **Diglycerol Dicarboxylate (DGC) synthesis using Conventional and Microwave Heating**

Maria Ioanna Lilikaki

**Supervisor:** Prof. Georgios Stefanidis

Athens, 2025



## Summary

Polyurethanes (PUs) are a wide and versatile category of polymers with applications including use in coatings as binders and thickeners, in food packaging, printing inks, and as fire-retardant barriers in wood treatments. However, since their introduction in 1947, their industrial synthesis largely relies on isocyanates (-NCO), which are highly toxic compounds associated with severe risks to human health and the environment. As a result, their use is increasingly restricted or even banned under current safety regulations such as the EU REACH Restriction, prompting the development of sustainable and safer synthetic alternatives.

The synthesis of environmentally friendly non-isocyanate polyurethanes (NIPUs) is gaining increasing attention as an alternative to conventional polyurethane production. Among various NIPU precursors, diglycerol dicarbonate (DGC), a bifunctional five-membered cyclic carbonate, stands out due to its renewable origin, structural suitability, and promising reactivity toward amines for the formation of polyhydroxyurethanes (PHUs). This is because diglycerol (DIG) is the simplest derivative of cheap glycerol, which is a by-product of biodiesel preparation.

This study investigates, for the first time, the synthesis of DGC via transesterification of DIG with dimethyl carbonate (DMC) under both conventional heating (CH) and microwave heating (MWH), with a particular emphasis on process intensification through MWH. The reaction is catalyzed using both homogeneous (NaOMe) and heterogeneous (CaO) basic catalysts and operates under autogenous pressure in batch systems. In contrast to previous studies, which typically employ CH under reflux conditions, this work explores a broader range of operational parameters, including catalyst type and loading, DMC:DIG molar ratio, and temperature.

Initially, DIG and DGC were characterized through FTIR, NMR, TGA, and dielectric analysis. These confirmed the successful formation of DGC and validated that the applied heating method did not affect its chemical structure. The dielectric properties analysis showed increased microwave compatibility as the reaction progresses due to the conversion of non-polar DMC into polar products, like DGC and methanol (MeOH), reinforcing the suitability of MWH for this system.

Isothermal screening revealed that MWH significantly enhances the reaction when CaO, as heterogeneous catalyst, is used, enabling it to match or exceed the performance of NaOMe, as a

homogeneous one. Response Surface Methodology (RSM) based on Central Composite Design (CCD) was implemented to systematically evaluate the effects of temperature, DMC:DIG molar ratio, and catalyst loading. Among these, temperature was identified as the most critical parameter, with elevated temperatures (especially 130–150 °C) resulting in substantial increases in DIG conversion and DGC yield, primarily through Arrhenius-driven kinetics and enhanced MeOH vapor-phase transfer. The DMC:DIG molar ratio was the second most influential parameter, with an optimum at ~6:1. Higher ratios led to performance decline, attributed to a drop in catalyst concentration caused by dilution when DMC volume increases. Additionally, under MWH reduced polarity of the reaction medium caused by the excess non-polar DMC negatively affects microwave heat dissipation. Catalyst loading had the least impact within the tested range.

Finally, to further optimize performance, a series of dynamic MWH experiments were conducted using temperature cycling (TC). These profiles aimed to expose the reaction mixture to short-term elevated temperatures while avoiding prolonged exposure that could lead to polyglycerol formation. Among the profiles tested, one particular TC strategy (210 °C for 1 min,  $T_{\min} = 130$  °C) resulted in 98% DIG conversion and 73% DGC yield, while keeping PG formation to a minimum (7%). This profile also achieved substantial reductions in both reaction time (–78%) and energy consumption (–71%) compared to isothermal CH. These results demonstrate the benefit of transient MWH conditions over static heating in both reaction performance and energy efficiency.

Keywords: Diglycerol Dicarboxylate, Transesterification, Heating methods, Microwave heating, Conventional Heating Process intensification, Heat dissipation

## Περίληψη

Οι πολυουρεθάνες αποτελούν μια ευέλικτη και ευρέως χρησιμοποιούμενη κατηγορία πολυμερών με εφαρμογές που περιλαμβάνουν επιστρώσεις ως συνδετικά και πηκτικά μέσα, συσκευασίες τροφίμων, μελάνια εκτύπωσης, καθώς και πυροπροστατευτικά φράγματα στην επεξεργασία ξύλου. Ωστόσο, από την καθιέρωσή τους το 1947, η βιομηχανική τους σύνθεση βασίζεται σε μεγάλο βαθμό στη χρήση ισοκυανίων (-NCO), τα οποία είναι ιδιαίτερα τοξικές ενώσεις, με σοβαρές επιπτώσεις για την ανθρώπινη υγεία και το περιβάλλον. Επομένως, η χρήση τους περιορίζεται αυστηρά ή και απαγορεύεται σύμφωνα με τους σύγχρονους κανονισμούς ασφαλείας, όπως ο κανονισμός EU REACH, γεγονός που οδηγεί στην ανάγκη ανάπτυξης βιώσιμων και ασφαλέστερων συνθετικών εναλλακτικών.

Η σύνθεση περιβαλλοντικά φιλικών μη-ισοκυανικών πολυουρεθανών (Non-Isocyanate Polyurethanes, NIPUs) συγκεντρώνει ολοένα και μεγαλύτερο ερευνητικό ενδιαφέρον ως εναλλακτική προσέγγιση έναντι της κλασικής παραγωγής πολυουρεθανών. Μεταξύ των διαφόρων πρόδρομων ενώσεων NIPUs, η διανθρακική διγλυκερόλη (Diglycerol Dicarboxylate, DGC), ξεχωρίζει λόγω της ανανεώσιμης προέλευσής της, της δομικής καταλληλότητας και της ικανότητάς της να αντιδρά με αμίνες για τον σχηματισμό πολυυδροξυουρεθανών (PHUs). Η διγλυκερόλη (DIG) μάλιστα αποτελεί το απλούστερο παράγωγο της φθηνής γλυκερόλης, ενός υποπροϊόντος της παραγωγής βιοντίζελ.

Η παρούσα μελέτη διερευνά για πρώτη φορά τη σύνθεση DGC μέσω της αντίδρασης μετεστεροποίησης της διγλυκερόλης με ανθρακικό διμεθύλιο (DMC), υπό συνθήκες αυτόκλειστου αντιδραστήρα και εφαρμογή είτε συμβατικής (CH) είτε μικροκυματικής θέρμανσης (MWH), με έμφαση στη διερεύνηση στρατηγικών ενίσχυσης της διαδικασίας μέσω των μικροκυμάτων. Η αντίδραση καταλύεται από βασικούς ομογενείς (NaOMe) και ετερογενείς (CaO) καταλύτες.

Σε αντίθεση με προηγούμενες μελέτες που εφαρμόζουν κυρίως συμβατική θέρμανση υπό συνθήκες αναβρασμού, το παρόν έργο εξετάζει ευρύτερες παραμέτρους λειτουργίας, όπως το είδος και η ποσότητα του καταλύτη, η αναλογία DMC:DIG και η θερμοκρασία. Αρχικά, οι ενώσεις DIG και DGC χαρακτηρίστηκαν με FTIR, NMR, TGA και ανάλυση διηλεκτρικών ιδιοτήτων. Επιβεβαιώθηκε η επιτυχής σύνθεση του DGC, χωρίς επίδραση από τη μέθοδο θέρμανσης στη χημική του δομή. Η ανάλυση διηλεκτρικών ιδιοτήτων έδειξε αύξηση της μικροκυματικής

συμβατότητας καθώς προχωρά η αντίδραση, λόγω μετατροπής του μη-πολικού DMC σε πολικά προϊόντα (DGC και MeOH), υποστηρίζοντας την καταλληλότητα για MWH.

Αποδείχθηκε ότι η μικροκυματική θέρμανση ενισχύει σημαντικά την απόδοση του CaO, επιτρέποντάς του να προσεγγίσει ή να υπερβεί τις επιδόσεις του NaOMe. Με την βοήθεια της μεθοδολογίας απόκρισης επιφάνειας (Response Surface Methodology, RSM) και χρήση Κεντρικού Σύνθετου Σχεδιασμού (CCD), επιτεύχθηκε συστηματική αξιολόγηση της επίδρασης των τριών παραμέτρων. Διαπιστώθηκε ότι η θερμοκρασία είναι ο πιο κρίσιμος παράγοντας, καθώς η αύξηση στους 130–150°C οδηγεί σε σημαντική βελτίωση της μετατροπής της DIG και της απόδοσης DGC. Ο μοριακός λόγος DMC:DIG ήταν ο δεύτερος πιο σημαντικός παράγοντας, με ιδανικό σημείο το 6:1, ενώ υψηλότεροι λόγοι οδήγησαν σε μείωση απόδοσης λόγω υποβάθμισης της συγκέντρωσης καταλύτη στο δείγμα. Στα μικροκύματα επίδραση είχε και η μείωση της πολικότητας του δείγματος. Η ποσότητα του καταλύτη είχε τη μικρότερη επίδραση στο εξεταζόμενο εύρος.

Για περαιτέρω ενίσχυση της απόδοσης, πραγματοποιήθηκε σειρά πειραμάτων με μικροκυματική θέρμανση, αυτή τη φορά υπό συνθήκες θερμικού κύκλου (Temperature Cycling, TC). Τα προφίλ στόχευαν στην παροδική έκθεση του μίγματος σε υψηλές θερμοκρασίες με ταυτόχρονη αποφυγή υπερβολικής παραγωγής πολυγλυκερόλης. Μεταξύ των σεναρίων, το TC με  $T_{\max} = 210\text{ }^{\circ}\text{C}$  για 1 λεπτό και  $T_{\min} = 130\text{ }^{\circ}\text{C}$  πέτυχε 98% μετατροπή DIG και 73% απόδοση DGC, με μόλις 7% δημιουργία πολυγλυκερόλης. Παράλληλα, ο χρόνος αντίδρασης και η ενεργειακή κατανάλωση μειώθηκαν κατά 78% και 71%, αντίστοιχα, σε σύγκριση με την ισοθερμική CH.

Λέξεις-κλειδιά: Διανθρακική Διγλυκερόλη, Μετεστεροποίηση, Μέθοδοι θέρμανσης, Θέρμανση με μικροκύματα, Συμβατική θέρμανση, Εντατικοποίηση διεργασίας, Απαγωγή θερμότητας

## Contents

Summary .....	3
Περίληψη .....	5
Figures and Tables .....	9
Introduction.....	11
1.1 Polyurethanes: Structure, Applications, and Industrial Relevance.....	11
1.2 Synthetic Routes to NIPUs: Classification and Comparative Assessment.....	12
1.3 Focus on the Polyaddition Route and the role of Bis-cyclic Carbonates.....	16
1.4 The Case for Diglycerol Dicarboxylate: A Renewable and Bifunctional Monomer .....	18
1.5 Reaction Scheme and Mechanistic Considerations in DGC Synthesis .....	19
1.6 Catalyst Strategies for Transesterification.....	21
1.7 Microwave Heating in Glycerol-Based Transesterification: Toward Process Intensification...	22
1.8 Scope and Research Motivation .....	23
Experimental.....	24
2.1 Materials .....	24
2.2. Apparatus and Synthesis Procedure.....	24
2.2.1 Isothermal operation .....	26
2.2.2 Temperature Cycling.....	28
2.3. Postreaction Procedure.....	29
2.4 Analytical Methods.....	30
2.4.1 High-performance liquid chromatography (HPLC).....	30
2.4.2 Fourier Transform Infrared Spectroscopy (FT-IR) .....	30
2.4.3 Nuclear Magnetic Resonance (NMR).....	31
2.4.4 Energy Cost Analysis.....	31
2.4.5 Thermogravimetric Analysis (TGA).....	31
2.4.6 Dielectric properties measurement.....	32
Results.....	33
3.1 Reactant and product characterization .....	33
3.1.1 FT-IR analysis.....	33
3.1.2 <sup>1</sup> H NMR analysis .....	35
3.1.3 TG analysis .....	36
3.1.4 Dielectric properties .....	36
3.2 Effect of stirring.....	37
3.3 Homogeneous vs heterogeneous catalysis .....	38
3.3.1 Heterogeneous catalysis.....	38

3.3.2 Homogeneous catalysis.....	40
3.3.3 Comparison.....	41
3.4 Isothermal operation.....	41
3.4.1 Catalyst loading.....	42
3.4.2 DMC:DIG molar ratio.....	44
3.4.3 Temperature.....	46
3.4.4 Overall comparison.....	48
3.5 Dynamic operation.....	50
Conclusions.....	53
References.....	56
Acknowledgements.....	59
List of Abbreviations.....	60

## Figures and Tables

Figure 1: NIPUs synthesis routes, as presented by Mundo .....	12
Figure 2: Schematic representation of the polycondensation route in NIPU synthesis, as presented by Balla et al. ....	13
Figure 3: NIPU synthesis through polymerization of cyclic urethane, as presented by Balla et al. ....	14
Figure 4: . Schematic representation of rearrangement NIPU synthesis reaction, as presented by Balla et al. ....	14
Figure 5: Schematic representation of polyaddition reaction, as presented by Balla et al. ....	15
Figure 6: Overview of synthetic routes to polyurethanes. ....	16
Figure 7: Paths for the creation of NIPUs from monofunctional and bifunctional monomers.....	17
Figure 8: Synthesis of 5-Membered Bis-Cyclic Carbonates, as presented by Maisonneuve et al.	18
Figure 9: Reaction scheme from reactants to intermediates .....	19
Figure 10: Reaction scheme from intermediates to final products .....	20
Figure 11: Reaction scheme of side reaction .....	20
Figure 12: CCD design for DGC production.....	25
Figure 13: Experimental setup used for CH: a 50mL stainless steel reactor (1) placed on top of a magnetic/heating plate (2). PT1000 temperature sensor (3) for temperature monitoring, manometer (4) and pressure indicator (5) for pressure monitoring, and vapor sample valve (6).	26
Figure 14: Experimental setup used for MWH: a 200W solid state generator (1) was connected via a coaxial cable (2) to an MW cavity (3), which contains the 50mL borosilicate glass reactor (4), and a magnetic plate (5) was placed under the cavity. An IR pyrometer (6) was connected to the generator for temperature monitoring, while the pressure was indicated by a manometer (7) and a pressure indicator (8). A sample for the vapor phase was retrieved via a vapor sample valve (9). ....	27
Figure 15: Anton Paar Monowave 300 MW oven. ....	29
Figure 16: FT-IR Analysis System. ....	30
Figure 17: Uni-T UT230B power meter .....	31
Figure 18: Top: FT-IR spectra of synthesized DGC, Down: FT-IR spectra of DGC from literature. ....	34
Figure 19: <sup>1</sup> H NMR spectra of synthesized DGC, Down: <sup>1</sup> H NMR spectra of DGC from literature. ....	35
Figure 20: TG curve of DIG. ....	36
Figure 21: Loss tangent as a function of temperature/ dielectric properties.....	36
Figure 22: Effect of stirring on conversion and yield results/ heterogeneous catalyst .....	37
Figure 23: Effect of stirring on conversion and yield results/ homogeneous catalyst .....	38
Figure 24: Comparison of DIG conversion (%) and DGC yield (%) under isothermal conditions for CH and MWH/ heterogeneous catalysis .....	39
Figure 25: Evolution of pressure through reaction time for CH and MWH/ heterogeneous catalysis.....	39

Figure 26: Comparison of DIG conversion (%) and DGC yield (%) under isothermal conditions for CH and MWH/ heterogeneous catalysis .....	40
Figure 27: Comparison of conversion of DIG and yield of DGC for CH and MWH/ both types of catalyst .....	41
Figure 28: DIG conversion and DGC yield for experiments with DMC: DIG MR of 6:1, temperature of 130 °C, and reaction time of 2 hours. ....	42
Figure 29: Autogenous pressure for experiments with DMC: DIG MR of 6:1, temperature of 130 °C, and reaction time of 2 hours. ....	43
Figure 30: Relative MeOH vapor phase for experiments with DMC: DIG MR of 6:1, temperature of 130 °C, and reaction time of 2 hours. ....	44
Figure 31: DIG conversion/DGC yield for experiments at 130 °C for 2 hours using 1.05% w/w <sub>DIG</sub> CaO.....	45
Figure 33: DIG conversion and DGC yield for experiments using CaO at 1.05% w/w <sub>DIG</sub> , DMC:DIG MR 6:1, and reaction time of 2 hours .....	46
Figure 34: Relative MeOH vapor phase for experiments using CaO at 1.05% w/w <sub>DIG</sub> , DMC:DIG MR 6:1, and reaction time of 2 hours .....	47
Figure 35: Polyglycerol yield for experiments using CaO at 1.05% w/w <sub>DIG</sub> , DMC:DIG MR 6:1, and reaction time of 2 hours.....	47
Figure 37: Overview of results for DIG conversion under CH and MWH .....	49
Figure 38: Overview of results for DGC yield under CH and MWH.....	50
Figure 39: Temperature cycling profiles. ....	51
Table 1: Reaction conditions for CH and MWH experiments .....	25
Table 2: Reaction conditions for Temperature cycling experiments.....	28
Table 3: Results for temperature cycling experiments and CH experiments .....	51

# Introduction

## 1.1 Polyurethanes: Structure, Applications, and Industrial Relevance

Polyurethanes (PUs) represent a highly versatile and widely utilized class of polymers, defined by the presence of urethane linkages in their macromolecular chains. Traditionally, PUs are synthesized through the reaction between polyols and diisocyanates, resulting in materials that can be chemically and mechanically tailored to meet a broad spectrum of application demands. This adaptability, in terms of stiffness, elasticity, chemical resistance, and durability, has emphasized the need for PUs across many different industries.<sup>1</sup>

Since their introduction in 1947, the applications of PUs have expanded, and nowadays they span diverse sectors. Flexible PU foams are heavily employed in consumer products such as mattresses, automotive seating, and footwear, where cushioning and comfort are prioritized. On the other hand, rigid PU foams play a key role in construction and refrigeration as they present exceptional thermal insulation properties. For instance, they are being widely used in panels, appliances, and building insulation. Furthermore, elastomeric PUs offer high resilience and resistance, making them ideal for use in wheels, tires, seals, and gaskets. The CASE segment (Coatings, Adhesives, Sealants, and Elastomers) takes advantage of PU's excellent surface adhesion, chemical resistance, and flexibility, supporting applications in protective coatings, industrial adhesives, and sealants.<sup>2</sup>

In addition to traditional markets, the rising sector of biomedical applications of PUs has gained importance. Medical-grade PUs are now used in wound dressings, implantable devices, and drug delivery systems, thanks to their biocompatibility and controlled mechanical properties.<sup>3</sup>

Despite their popularity in daily life necessities, traditional polyurethane production methods present challenges, with the use of toxic and hazardous diisocyanates as the most important one. Nowadays, with sustainable chemistry development and new regulations, research groups and industries have to replace hazardous chemicals and harsh reaction conditions with greener intermediates and processes. Exposure to isocyanates during manufacturing brings concerns related to environmental and end-of-life impacts and has shifted research into safer alternatives. One of the most promising avenues has been the development of non-isocyanate polyurethanes (NIPUs).<sup>4</sup>

## 1.2 Synthetic Routes to NIPUs: Classification and Comparative Assessment

NIPUs avoid the use of isocyanates (-NCO) entirely. Except for the toxicity concerns that these compounds solve, NIPUs also offer potential advantages in terms of thermal stability, solvent resistance, and sustainability. For instance, many of the monomers used in NIPU synthesis are accessible from bio-based feedstocks.

NIPUs can be synthesized via several distinct reaction mechanisms, each of which offers distinct characteristics. Their differences might be noticed in structural control, scalability, and sustainability. While multiple classifications exist in the literature, the main routes converge around four synthetic strategies: polyaddition of cyclic carbonates with amines, polycondensation reactions, ring-opening polymerization (ROP) of cyclic urethanes or carbamates, and rearrangement reactions involving the generation of isocyanates.<sup>5</sup>

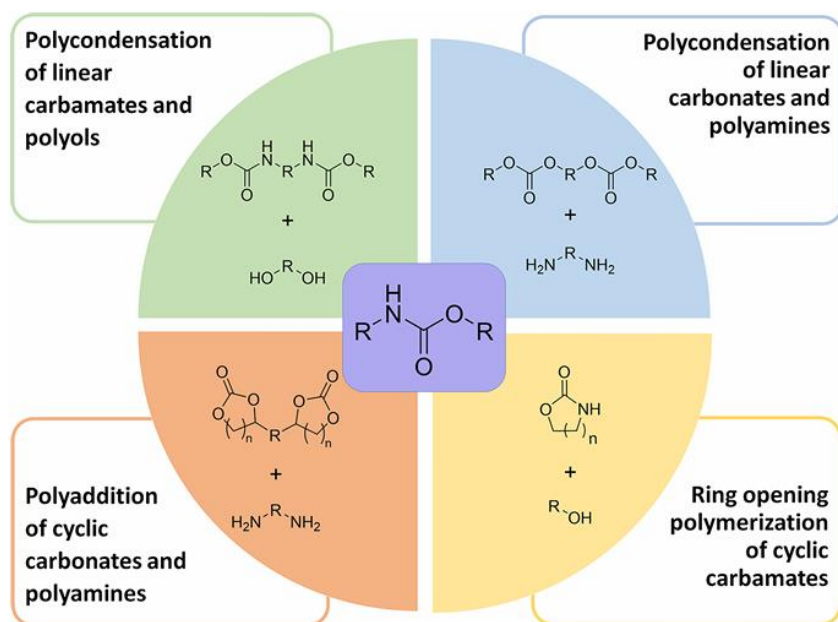


Figure 1: NIPUs synthesis routes, as presented by Mundo

The first route involves polycondensation reactions, including the transurethanization of linear activated carbamates with polyols or diamines. These processes form urethane linkages through step-growth polymerization, typically releasing alcohol or water as by-products.<sup>5</sup> Even though polycondensation offers advantages like the ability to use renewable feedstocks and well-known

reaction frameworks, it also presents limitations. The most crucial problems are the difficult removal of side products, and that it often requires high temperatures to proceed efficiently. Some versions of this method still involve precursors derived from phosgene, isocyanates or other hazardous reagents, also raising toxicity and health concerns.<sup>6,7</sup>

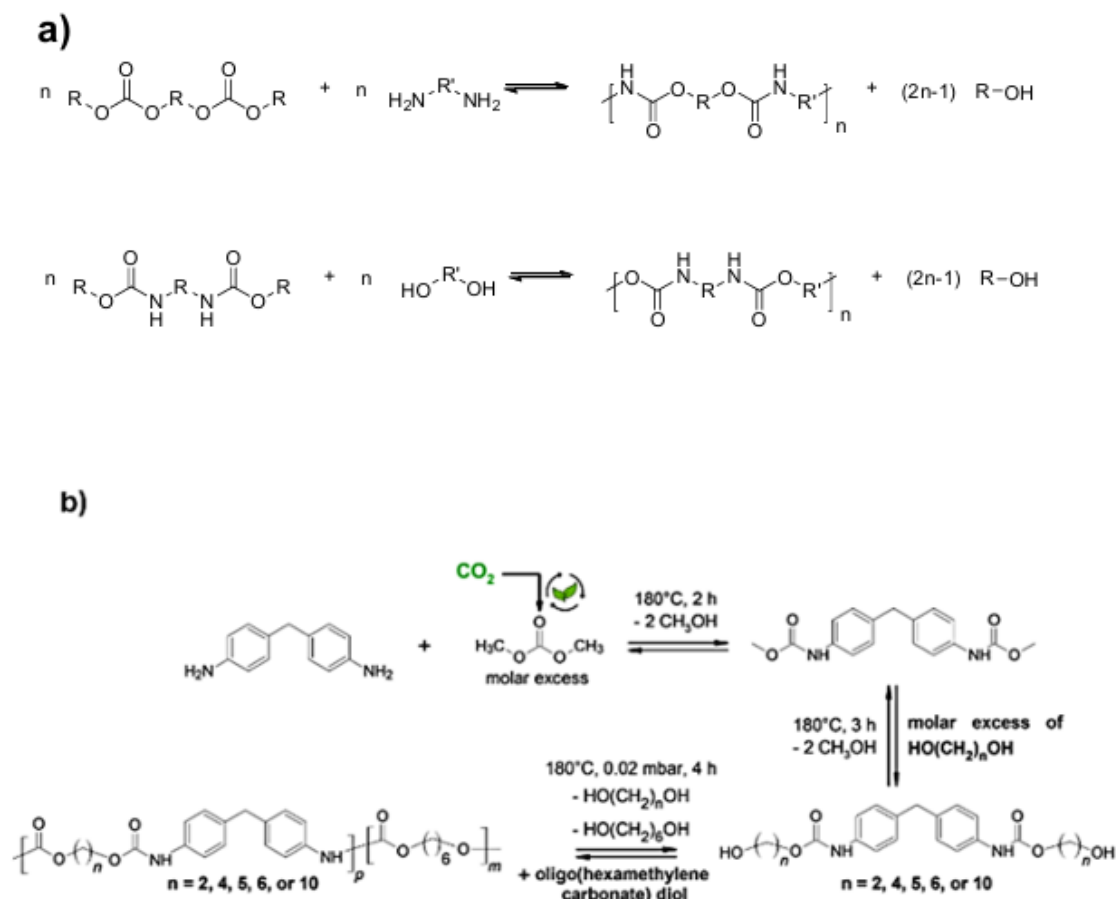


Figure 2: Schematic representation of the polycondensation route in NIPU synthesis, as presented by Balla et al.

The second synthetic route is the ring-opening polymerization (ROP) of cyclic urethanes or aliphatic 6-7- membered cyclic carbamates. This scheme is attractive because it can generally proceed without the generation of by-products, and in some cases, the resulting polymers show promising mechanical and thermal properties. However, ROP typically requires elevated temperatures, and many cyclic urethane monomers are derived from phosgene or involve significant synthetic effort. As a result, this method remains underexplored in industrial settings, although it holds potential for high-performance applications as greener routes are arising.<sup>6,7</sup>

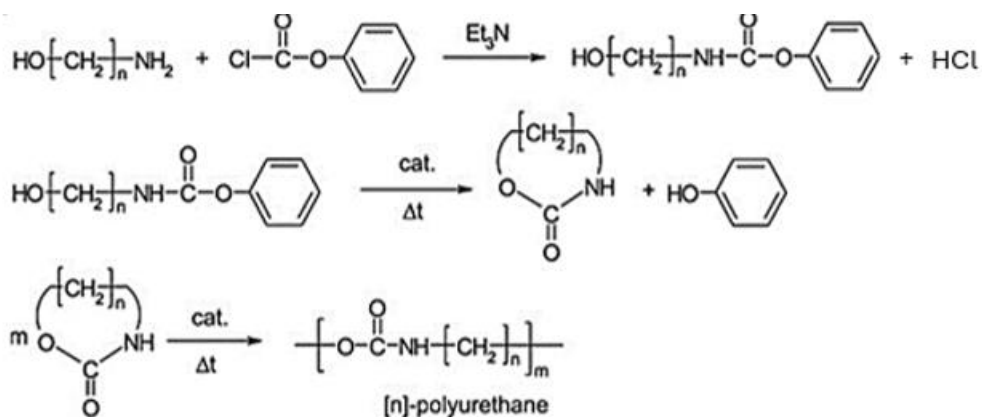


Figure 3: NIPU synthesis through polymerization of cyclic urethane, as presented by Balla et al.

The rearrangement reactions, such as those of Curtius, Hofmann, or Lossen, offer another route to polyurethane structures. These mechanisms utilize precursors like acyl azides, carboximides, or hydroxamic acids, which produce isocyanates in situ. So, even though they technically avoid the use of commercial diisocyanates, they still produce them transiently and require highly toxic intermediates, which pose challenges in terms of safety, regulation, and sustainability. In order to overcome these problems, studies have been investigating the possibility of using the rearrangement of dimethyl carbonate (DMC).<sup>6,7</sup>

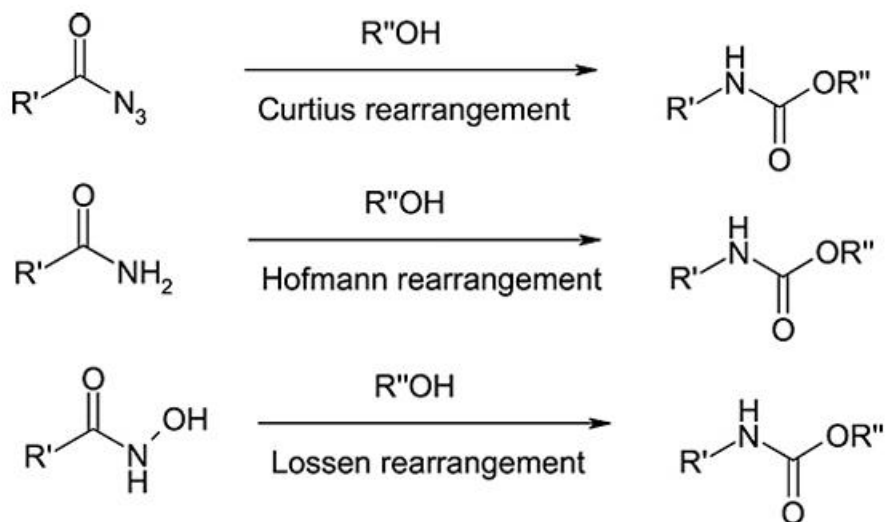


Figure 4: Schematic representation of rearrangement NIPU synthesis reaction, as presented by Balla et al.

Lastly, the most widely investigated route is the polyaddition of cyclic carbonates and amines, which yields polyhydroxyurethanes (PHUs), a name that comes from the primary or secondary hydroxyl groups formed. Within the polyaddition route, the synthesis of NIPUs proceeds through a two-step process involving the formation of cyclic carbonate oligomers, followed by their step-growth reaction with diamines or polyamines, as shown on Figure 5. This method is widely recognized as the most efficient and sustainable route because it fully eliminates the use of phosgene. Simultaneously, PHUs show significantly improved stability compared to conventional PUs, and improved chemical and thermal resistance.<sup>6,7</sup>

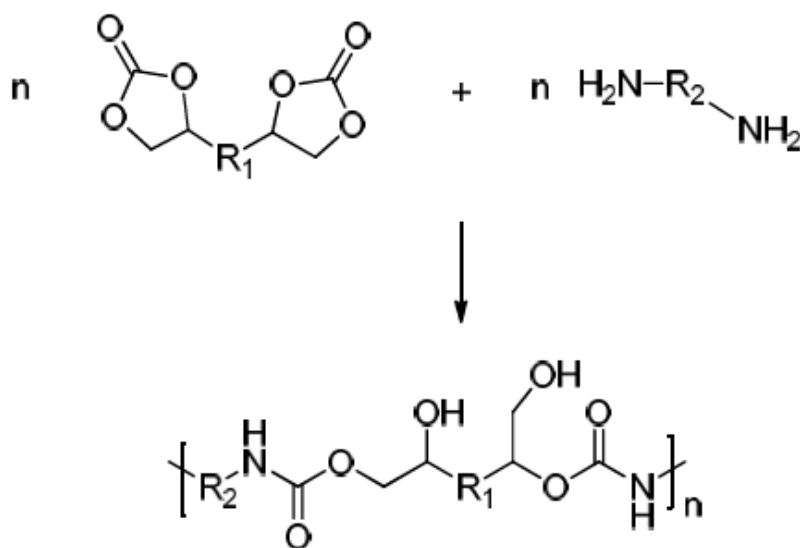


Figure 5: Schematic representation of polyaddition reaction, as presented by Balla et al.

In conclusion, while each synthetic route to NIPUs presents specific advantages, the polyaddition of cyclic carbonates and amines currently stands out as the most industrially feasible and environmentally aligned method.

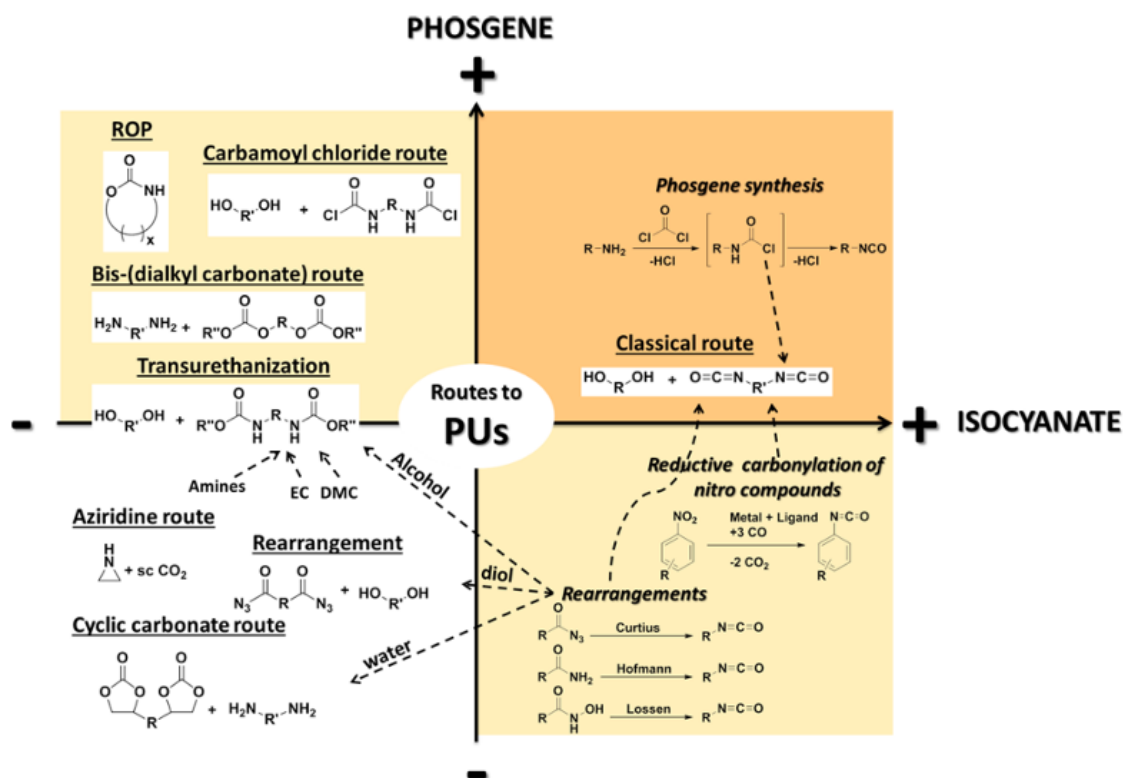


Figure 6: Overview of synthetic routes to polyurethanes, as presented by Maisonneuve

### 1.3 Focus on the Polyaddition Route and the role of Bis-cyclic Carbonates

Despite the advantages mentioned, the polyaddition route can also present some limitations, like the production of low molecular weight PHUs, especially in mild temperatures. To overcome this challenge, differentiations in monomer structure, stoichiometry, and reaction temperature can be explored.<sup>7</sup>

More specifically, the broader classification of cyclic carbonates, relevant to NIPU synthesis through the polyaddition route, distinguishes mono-cyclic carbonates (MCCs), such as glycerol carbonate, and bis-cyclic carbonates like diglycerol decarbonate (DGC). MCCs possess a single carbonate ring and are inherently monofunctional, meaning they terminate polymer chains and result in oligomeric or low molecular weight PHUs.<sup>8</sup> In contrast, BCCs contain two cyclic carbonates, typically at terminal positions, enabling chain extension. This allows to produce high-molecular-weight linear PHUs or lightly crosslinked networks, depending on stoichiometry and reaction conditions.<sup>4</sup>

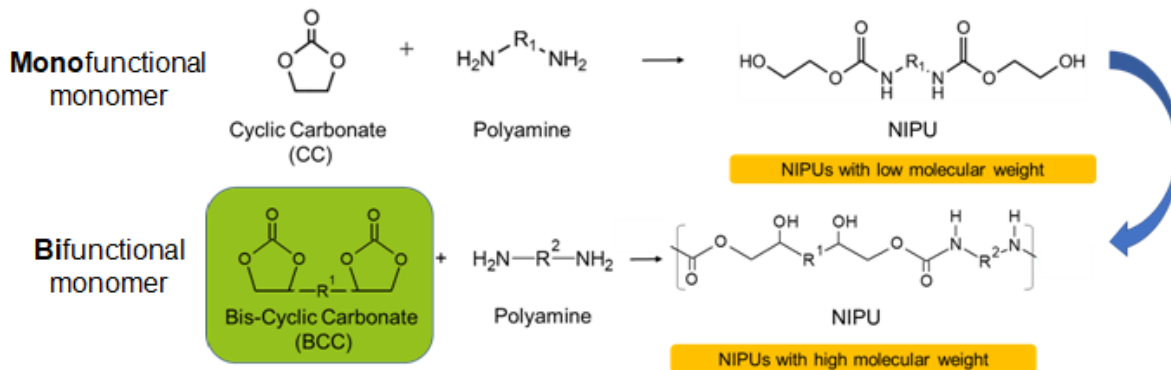


Figure 7: Paths for the creation of NIPUs from monofunctional and bifunctional monomers.

Generally, MCCs or BCCs with five- or six-membered cyclic carbonate rings employed in this route can be synthesized via a range of chemistries. However, five-membered carbonates are preferred due to their greater thermodynamic stability, synthetic accessibility under mild conditions, and resistance to homopolymerization, which makes them more suitable for controlled NIPU synthesis.<sup>9</sup>

Focusing on the production of 5-membered BCCs, many different pathways for their synthesis can be selected, including the cycloaddition of carbon dioxide to epoxides, transesterification of diols with dialkyl carbonates, oxidative carbonylation, and routes involving halohydrins, as illustrated in Figure 8. Each pathway presents specific advantages and limitations concerning precursor availability, energy input, catalytic requirements, and by-product generation.<sup>4</sup>

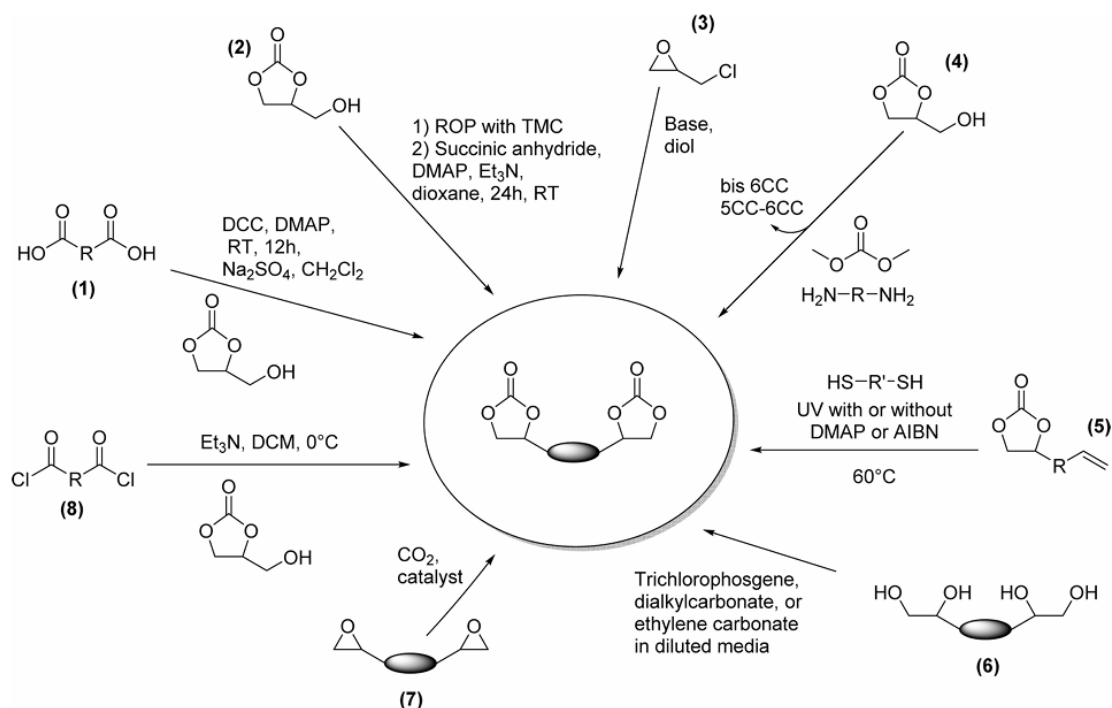


Figure 8: Synthesis of 5-Membered Bis-Cyclic Carbonates, as presented by Maisonneuve et al.

The DGC molecule produced via diglycerol transesterification is a great example of a highly efficient five-membered BCC. The subsequent polyaddition of DGC with aliphatic or aromatic diamines proceeds cleanly, without toxic by-products, yielding high-performance polymers that exhibit enhanced mechanical and thermal properties and higher molecular weight.

## 1.4 The Case for Diglycerol Dicarboxylate: A Renewable and Bifunctional Monomer

Building on the relevance of five-membered BCCs for high-performance NIPU synthesis, DGC stands out not only because of its molecular structure but also for its renewable origin. Glycerol, which is a by-product of biodiesel production, has become increasingly abundant in recent years, with global output exceeding 1.5 million tons, far surpassing the current industrial demand. Diglycerol (DIG) is the simplest oligomeric derivative of glycerol, and it offers promising characteristics. It is widely applied in food, cosmetics (such as soaps and toothpaste), and chemical formulations, including printing inks.<sup>10</sup> At the same time, unlike glycerol, whose direct transesterification with DMC leads to monofunctional glycerol carbonate, DIG enables the formation of a bifunctional product, thereby overcoming the chain-terminating limitations MCCs.<sup>11</sup>

In addition, DIG possesses favorable properties like low volatility, high thermal stability, mechanical strength, and compatibility with solvent-free processing. These attributes not only facilitate its transformation into DGC under relatively mild transesterification conditions but also contribute to the environmental and economic aspects.<sup>10</sup>

Overall, DGC combines structural efficiency with bio-based accessibility, positioning it as a strategically important monomer for the development of isocyanate-free polyurethanes within a sustainable approach.

## 1.5 Reaction Scheme and Mechanistic Considerations in DGC Synthesis

As mentioned, the product of this experimental process, DGC, is typically prepared through a two-step transesterification process. The transesterification of DIG with DMC is reversible and is accompanied by the formation of an intermediate.<sup>12</sup>

The first step involves the reaction between DIG and dimethyl carbonate (DMC). This pathway proceeds under relatively mild thermal conditions, often in the presence of a catalyst, either heterogeneous or homogeneous.<sup>14</sup> In this step, the formation of diglycerol monocarbonate (DGMC), a mono-substituted cyclic carbonate intermediate, is achieved along with MeOH, as a co-product.<sup>15,16</sup>

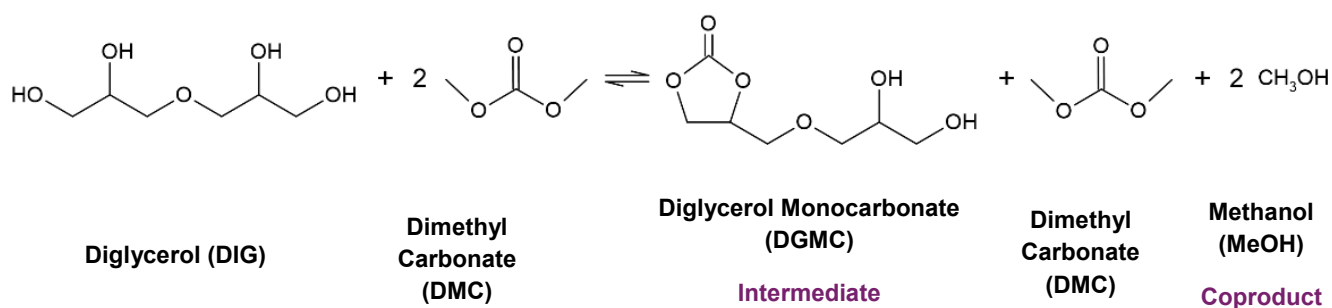


Figure 9: Reaction scheme from reactants to intermediates

In the next step, the intermediate is further transformed into the desired product of DGC, which is accompanied by the release of MeOH, the coproduct of the reaction. The overall process converts DIG (polyol) into a BCC by adding two hydroxyl groups with carbonate rings, allowing DGC to

function as a bifunctional monomer in the subsequent polyaddition with diamines to form high molecular weight PHUs.<sup>12</sup>

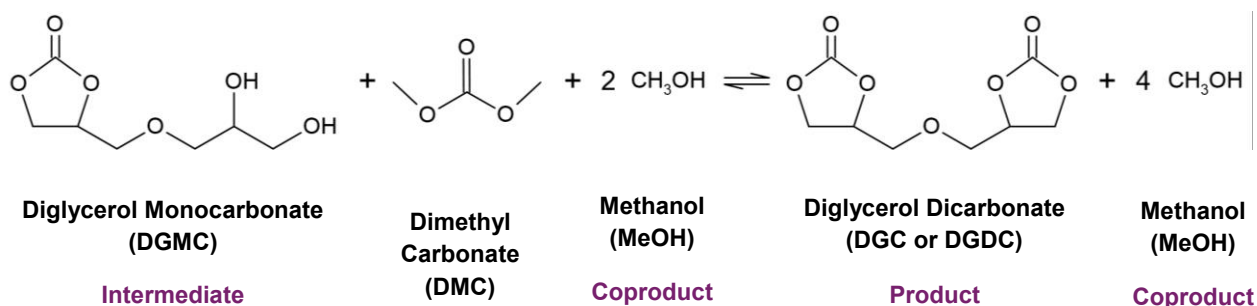


Figure 10: Reaction scheme from intermediates to final products

Simultaneously, a competing reaction is present, as DIG can be polymerized into polyglycerol (PG), which is an undesired, side product. Prolonged reaction times and higher temperatures favor further polymerization into longer-chain PGs. To prevent the undesired formation of higher PGs during DGC synthesis, it is essential to optimize reaction conditions carefully.<sup>16</sup>

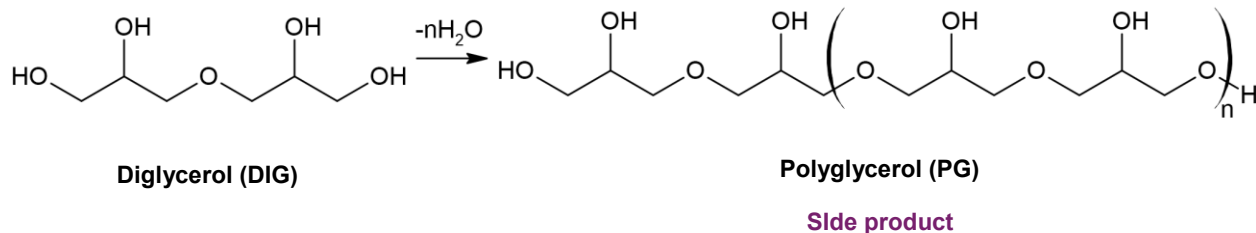


Figure 11: Reaction scheme of side reaction

So far, the reported studies of this reaction have implemented conventional heating (CH) methods, while microwave heating (MWH) systems remain largely unexplored. To be exact, the research has been conducted primarily under CH reflux conditions in relatively mild temperature conditions (<90 °C), instead of autogenous (>90 °C).<sup>10,11,13</sup>

Both homogeneous and heterogeneous catalysts have been explored, but the most predominant ones are homogeneous ones, like sodium methoxide (NaOMe) and potassium carbonate (K<sub>2</sub>CO<sub>3</sub>).<sup>10,11</sup> The achieved results indicated shorter reaction times and higher yields compared to CaO, but also present recovery challenges due to dissolution in the reaction medium.<sup>14</sup> In addition,

an increase in reaction time is interwoven with the formation of the intermediates and/or byproducts.<sup>12</sup>

Recent studies also suggest that if coproduct MeOH is eliminated by distillation, the conversion yield can be increased from 70% to 85% within 42 h, showing that there is an equilibrium shift to the right. This proves a potential correlation between the removal of MeOH and better process performance.<sup>14</sup>

Lastly, only one parametric study has been carried out to investigate the influence of how the DMC:DIG molar ratio (MR) and catalyst loading influence the reaction outcome; however, key results like conversion were not attained.<sup>13</sup>

## 1.6 Catalyst Strategies for Transesterification

As explained, the transesterification of DIG with DMC to produce DGC, as described in the reaction schemes above, is generally achieved using a catalyst. In addition to other process conditions, such as temperature and molar ratio, catalyst selection and loading play a vital role in optimizing the efficiency and selectivity of a reaction.<sup>17</sup>

For the process to be industrially feasible, the catalyst type should meet some basic criteria: it should be cheap and easy to separate from the product with simple purification steps, the yield of DGC should be high, and the reaction time should be short to allow efficient and cost-effective production.<sup>18</sup>

As demonstrated by Ochoa-Gómez et al. (2009), basic catalysts significantly outperform acidic ones in this type of reaction systems. Acid catalysts, whether homogeneous (e.g., sulfuric acid) or heterogeneous (e.g., ion exchange resins), exhibit poor activity, with low conversion and yield, even after extended reaction times. This is explained primarily due to kinetic limitations and ineffective cyclization steps.

On the other hand, basic catalysts facilitate the nucleophilic attack on the carbonyl carbon of DMC, making them a more suitable choice. Usually, high yields and conversions are observed under moderate temperatures, with catalytic performance correlating directly with basic strength.<sup>18</sup>

In the same study, a comparative analysis of homogeneous and heterogeneous basic catalysts revealed important distinctions in their performance for the transesterification of glycerol with DMC. Homogeneous catalysts, such as sodium and potassium methoxides or hydroxides, exhibited superior activity and selectivity, achieving high conversions and yields under relatively mild conditions. However, their solubility in the reaction medium complicates catalyst separation and limits reusability. In contrast, heterogeneous catalysts, including alkaline earth oxides like CaO and MgO, demonstrated lower but still significant catalytic activity. While requiring higher catalyst loadings and longer reaction times, they offer the advantage of easier recovery and potential reuse, making them more attractive for scalable industrial processes.

## 1.7 Microwave Heating in Glycerol-Based Transesterification: Toward Process Intensification

Although limited research exists on MWH in the transesterification of DIG, recent studies involving glycerol provide important insights into its potential for process intensification. The transesterification of glycerol with DMC has served as a model system to understand and evaluate the effects of MWH compared to CH, revealing notable advantages in terms of both efficiency and selectivity.<sup>19,20</sup>

More specifically, these studies have shown that microwave-assisted systems can achieve significantly faster reaction rates and improved catalyst performance under similar conditions. The interaction of microwave energy with polar reactants, such as glycerol and glycerol carbonate, enables rapid molecular activation. This effect contributes not only to faster conversion but also to better energy utilization, aligning with sustainability goals in green chemistry.<sup>20</sup>

Another key advantage of MWH lies in its ability to facilitate the removal of polar by-products like MeOH, which can otherwise limit conversion in equilibrium-based systems. By selectively accelerating the phase transition of low-boiling products, MWH can shift the reaction equilibrium, thereby increasing overall yield.<sup>19</sup> These characteristics are particularly valuable in systems involving polar reactants and products, such as DIG, DGC, and MeOH.

## 1.8 Scope and Research Motivation

Despite the growing interest in NIPU precursors, no prior work has systematically examined the effects of microwave irradiation on this reaction. To address this gap, this study will focus on the influence of key process variables. These include catalyst type and loading, reaction temperature, DMC:DIG molar ratio (MR).

In the context of the current study, the technique of MWH will be explored as a way of enhancing the transesterification of DIG to improve conversion, reduce reaction time, and support greener process conditions. For the comparison to be complete, parameter characteristics and behavior are tested under both MWH and CH.

By focusing on conversion, yield, and reaction time, this work seeks to assess the potential of MWH to enable more efficient, scalable, and greener synthesis routes for DGC and intensify the process.

# Experimental

## 2.1 Materials

DIG (>80% purity) was obtained from BIOSYNTH. DMC/ Extra Dry, Acroseal (99+% purity), CaO (99.95% purity on a metals basis) and NaOMe, used as the reaction's catalyst, and dimethyl sulfoxide-d<sub>6</sub> (DMSO-d<sub>6</sub>, ≥99.5% purity), used as NMR solvent, were purchased from Thermo Scientific. Methanol (MeOH, ≥99.8% purity), potassium bromide (KBr, spectroscopy grade), were purchased from Fisher Scientific. Finally, ultrapure water (18.2MΩcm) was used as a solvent and mobile phase for high-performance liquid chromatography (HPLC) analyses. All chemicals were used without further purification.

## 2.2. Apparatus and Synthesis Procedure

The transesterification reaction examined in this study, involving DIG and DMC, has already been presented in the introductory part in Figures 9 and 10. In brief, this reaction leads to the formation of DGC as the target product, with MeOH released as a co-product and DGMC acting as the main intermediate. PG may also form as a by-product under certain conditions through etherification pathways.

In order to explore the differences, two basic catalysts were evaluated: one homogeneous and one heterogeneous. Firstly, sodium methoxide (NaOMe) was selected as the homogeneous catalyst based on its strong basicity and extensive application in DGC synthesis. As mentioned, generally homogeneous systems enable rapid and efficient conversion, performing better than heterogeneous ones due to direct contact with reactants. However, they pose challenges in terms of catalyst separation and product purification.<sup>11</sup>

To complement this, calcium oxide (CaO) was chosen as a representative heterogeneous catalyst. CaO is generally acknowledged for its high catalytic activity in transesterification reactions and was reported to outperform other solid bases such as MgO and CaCO<sub>3</sub> under optimized conditions.<sup>18</sup> Some of the advantages include low cost, availability, and easy recovery through simple filtration. However, CaO may suffer from deactivation due to air exposure, especially when it is reused across multiple cycles.

To systematically study the influence of key reaction parameters, a Central Composite Design (CCD) was employed. CCD is a widely used statistical experimental design methodology that enables efficient exploration of multivariable systems by minimizing the number of experimental runs required while still providing robust data for modeling and optimization.

In this study, CCD was applied to assess how catalyst loading, DMC:DIG MR, and temperature affect reaction performance under both CH and MWH. All experiments were conducted isothermally.

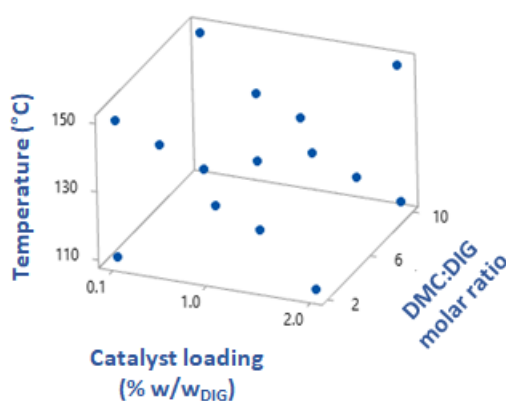


Figure 12: CCD design for DGC production

The parameter ranges used in the CCD study are summarized as follows:

<i>Central Composite Design (CCD)</i>	
<b>Reaction conditions</b>	
<b>Temperature (°C)</b>	110, 130, 150
<b>DMC:DIG molar ratio (MR)</b>	2:1, 6:1, 10:1
<b>Catalyst loading (% w/wDIG)</b>	0.1, 1.05, 2
<b>Reaction time (h)</b>	1, 2

Table 1: Reaction conditions for CH and MWH experiments

This experimental matrix made an investigation of the reaction system possible, offering insight into how each parameter influences DGC formation and overall process efficiency under both heating modes.

## 2.2.1 Isothermal operation

### 2.2.1.1 CH

CH experiments were conducted with the setup depicted in Figure 13. The setup consisted of a stainless steel 50mL reactor placed on a magnetic heating and stirring plate. The reaction temperature was measured using a PT1000 temperature sensor, while the pressure was indicated by a manometer and a pressure indicator. As mentioned, depending on the desired DMC: DIG molar ratio—2:1, 6:1, or 10:1—the masses of reactants were calculated to maintain a constant total volume across all experiments.

Firstly, the appropriate quantity of DIG was introduced into the reactor, followed by the weighed amount of catalyst (either NaOMe for homogeneous or CaO for heterogeneous catalysis). Subsequently, the calculated volume of DMC was added. Once sealed, the reactor was placed on the heating/ stirring plate, and the reaction proceeded under isothermal conditions (110, 130 or 150°C) for a duration of two hours. Once the reaction was complete, a vapor-phase sample was collected for analysis.

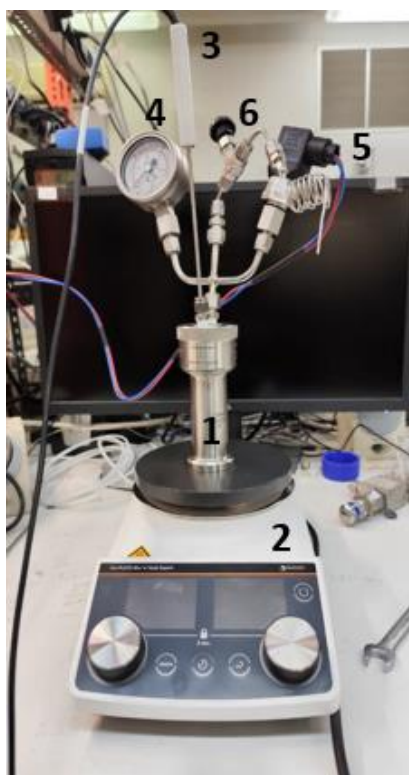


Figure 13: Experimental setup used for CH: a 50mL stainless steel reactor (1) placed on top of a magnetic/heating plate (2). PT1000 temperature sensor (3) for temperature monitoring, manometer (4) and pressure indicator (5) for pressure monitoring, and vapor sample valve (6).

### 2.2.1.2 MWH

The MWH experimental setup is shown in Figure 14. The 50mL borosilicate glass reactor was inserted in the MW cavity, which was connected via a coaxial cable to a solid-state generator (SSG) from Sairem Corporation (France). The SSG has a maximum output power of 200W and is adjustable in 1W steps, and works at 2.45GHz. The MW cavity is equipped with an adjustable stub for impedance matching. A stirring plate was placed beneath the MW cavity to ensure adequate mixing of the liquid solution. The reaction temperature was measured with an IR pyrometer, while the pressure was indicated by a manometer and a pressure indicator. The process that was followed for the MWH experiments was almost identical to that of CH mentioned above.

Reactant masses were calculated, weighted, and then added inside the reactor of Figure 14. After the completion of the reaction, a vapor phase sample was taken.

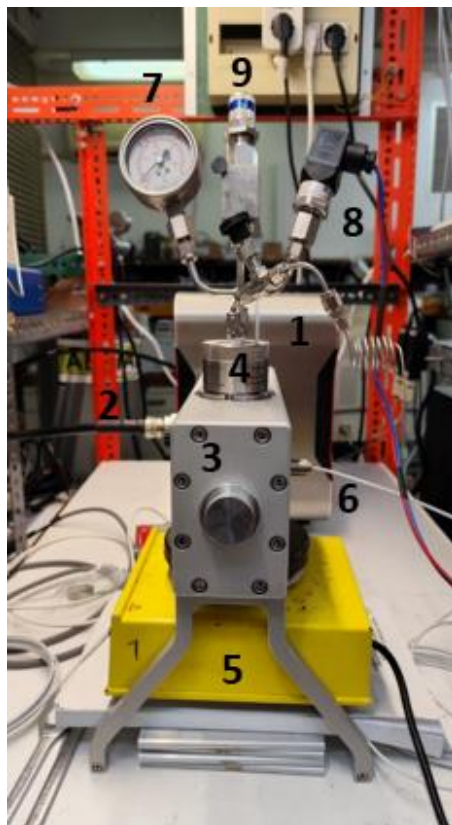


Figure 14: Experimental setup used for MWH: a 200W solid state generator (1) was connected via a coaxial cable (2) to an MW cavity (3), which contains the 50mL borosilicate glass reactor (4), and a magnetic plate (5) was placed under the cavity. An IR pyrometer (6) was connected to the generator for temperature monitoring, while the pressure was indicated by a manometer (7) and a pressure indicator (8). A sample for the vapor phase was retrieved via a vapor sample valve (9).

### 2.2.2 Temperature Cycling

Following the initial isothermal screening, the most promising catalyst loadings and DMC:DIG MRs were selected for further optimization under dynamic thermal conditions. To explore potential improvements in reaction performance, temperature cycling was applied using MWH instead of conventional isothermal profiles.

In this approach, the reaction temperature was alternated between defined maximum ( $T_{\max}$ ) and minimum ( $T_{\min}$ ) values over a set number of cycles. The goal was to promote reaction progress by periodically increasing temperature to accelerate transesterification kinetics and lowering it to reduce side reactions or thermal degradation. Each cycle included a specified holding time at  $T_{\max}$  and  $T_{\min}$ .

The experiments were conducted under a range of conditions involving variations in peak temperature, holding time, catalyst loading, and DMC:DIG MR. Table 2 summarizes the experimental parameters used for temperature cycling:

Reaction conditions	
$T_{\max}$ (°C)	170, 190, 210
$T_{\min}$ (°C)	110, 130
Holding time (min)	1, 3, 5
Number of Cycles	3

*Table 2: Reaction conditions for Temperature cycling experiments*

This dynamic heating strategy was designed to evaluate whether temperature modulation could enhance DGC yield and DIG conversion under microwave-assisted conditions compared to static isothermal operation. For the temperature cycling experiments, an Anton Paar Monowave 300 MW oven was used, which has a built-in pressure sensor and a FO for temperature measurement.



Figure 15: Anton Paar Monowave 300 MW oven.

### 2.3. Postreaction Procedure

Upon completion of the reaction, the mixture was allowed to cool, after which the catalyst was separated by vacuum filtration. The remaining volatile components (unreacted DMC and MeOH produced as a co-product) were removed under reduced pressure using a rotary evaporator. This left behind the residual reaction mixture, consisting primarily of unreacted DIG, DGMC as an intermediate, the desired product, DGC, and the side product, polyglycerol.

The vapor sample and a sample of the residual mixture were collected and analyzed by high-performance liquid chromatography (HPLC) to determine the concentrations of DMC, MeOH and DIG, DGMC, DGC, and PG, respectively. These measurements were used to calculate both the conversion of DIG and the yield of DGC.

The conversion of DIG was calculated using the equation:

$$\text{Conversion (\%)} = \frac{\text{moles of DIG reacted}}{\text{initial moles of DIG}} * 100\%, \text{ Eq. 1}$$

The yield of DGC was calculated as:

$$\text{Yield (\%)} = \frac{\text{moles of DGC obtained}}{\text{moles of DGC theoretically possible}} * 100\%, \text{ Eq. 2}$$

Accordingly, the yields of DGMC and PG were also calculated.

## 2.4 Analytical Methods

### 2.4.1 High-performance liquid chromatography (HPLC)

MeOH, DMC and DIG, DGC, DGMC, and PG concentrations in vapor and reaction samples, respectively, were determined using a high-performance liquid chromatography (HPLC) system (1260 Infinity series, Agilent Technologies), equipped with a PL aqua gel-OH 20 column and a refractive index (RI) detector. The analysis was carried out under isocratic conditions, using ultra-pure water as the mobile phase, with a constant flow rate of 1 mL/min.

### 2.4.2 Fourier Transform Infrared Spectroscopy (FT-IR)

The obtained product was qualitatively analyzed by FTIR spectroscopy using a Jasco FT/IR 6700 spectrometer applying the KBr method. Spectra were obtained with a resolution of  $2\text{cm}^{-1}$  and 32 scans per recording in the range of  $4000 - 400\text{cm}^{-1}$ . Prior to sample analysis, a background spectrum was recorded from the cell chamber to account for ambient environmental factors and baseline variations, ensuring that only the sample's absorbance is presented in the spectra.

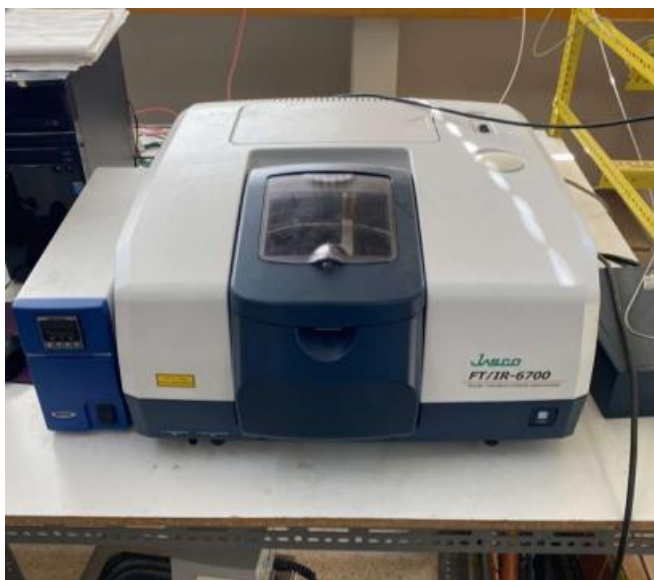


*Figure 16: FT-IR Analysis System.*

### 2.4.3 Nuclear Magnetic Resonance (NMR)

$^1\text{H}$  NMR and  $^{13}\text{C}$  NMR measurements were recorded on a Bruker Avance DRX 500MHz operating at 500.13MHz and 125.77MHz for  $^1\text{H}$  and  $^{13}\text{C}$  measurements, respectively. Samples were measured using DMSO- $d_6$  in an NMR tube of 5 mm OD and 700 mm length.

### 2.4.4 Energy Cost Analysis

Energy consumption during the synthesis was assessed using a Uni-T UT230B power meter. Measurements were taken for both heating methods to determine the energy required to raise the reactor temperature from room temperature to the reaction temperature (110-150°C), and to maintain that temperature throughout the reaction. These measurements enabled the calculation of total energy consumption for each experiment. While the analysis offers a useful first approximation of the energy demand associated with each method, it is important to note that these results are indicative and may vary significantly when scaled up to pilot or industrial levels.



Figure 17: Uni-T UT230B power meter

### 2.4.5 Thermogravimetric Analysis (TGA)

A Mettler Toledo TGA/DSC instrument was used to determine the safe temperature range for conducting the transesterification reaction without inducing thermal degradation or decomposition of the starting material, DIG. The atmosphere of the oven and balance chamber was filled with  $\text{N}_2$ , while the flow rate for the sample was 60 mL/min. Samples of 10mg were weighed in alumina crucibles and heated from 25 to 500°C at a heating rate of 10°C/min.

#### 2.4.6 Dielectric properties measurement

Dielectric constants and dielectric loss of the reaction compounds were measured using the cavity perturbation method.<sup>21</sup> A network analyzer (Anritsu MS2026C) connected to a PC and controlled by a self-written LabVIEW application was utilized. The samples were placed in a quartz tube with an internal diameter of 3mm and a length of up to 50mm. Measurements were conducted at a frequency of 2.45 GHz, across a temperature range of 25–85°C.

# Results

## 3.1 Reactant and product characterization

Before presenting the experimental results, preliminary analyses were conducted to confirm the identity and structural characteristics of the synthesized compounds and to determine the safe temperature range for carrying out the transesterification reaction. The three methods that were used to verify these were, as mentioned above, FT-IR,  $^1\text{H}$  NMR and TGA. Furthermore, dielectric property measurements were carried out to determine the dielectric constant ( $\epsilon'$ ) and dielectric loss factor ( $\epsilon''$ ) of the main reaction components (DIG, DMC, CaO, DGC, MeOH). These measurements serve as indicators of the compatibility of MWH with the individual reaction components.

### 3.1.1 FT-IR analysis

Figure 18 presents the FT-IR spectra of the synthesized DGC in order to elucidate its chemical structure and compare it with the literature. A clear and characteristic vibration band is observed at  $1791\text{ cm}^{-1}$ , which corresponds to the carbonyl group of the cyclic carbonate ( $\text{C}=\text{O}$ )<sup>22</sup>. Additionally, C–C and C–O stretching of the 2-hydroxyethyl chain of the product are identified at  $1151\text{ cm}^{-1}$  and  $1055\text{ cm}^{-1}$ , respectively.<sup>23</sup> Finally,  $1396\text{ cm}^{-1}$  corresponds to s- $\text{CH}_2$  bend,  $1174\text{ cm}^{-1}$  to s-CH bend, while the triplet of peaks at  $2880, 2925$ , and  $2993\text{ cm}^{-1}$  is due to the  $\text{CH}_2/\text{CH}$  vibrations of the cyclic carbonate.<sup>24</sup>

The FT-IR spectra of DGC synthesized showed no differences in peak positions or intensities from those in the literature, confirming the successful synthesis of DGC.

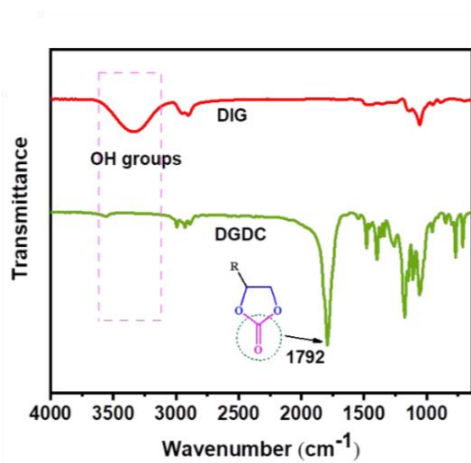
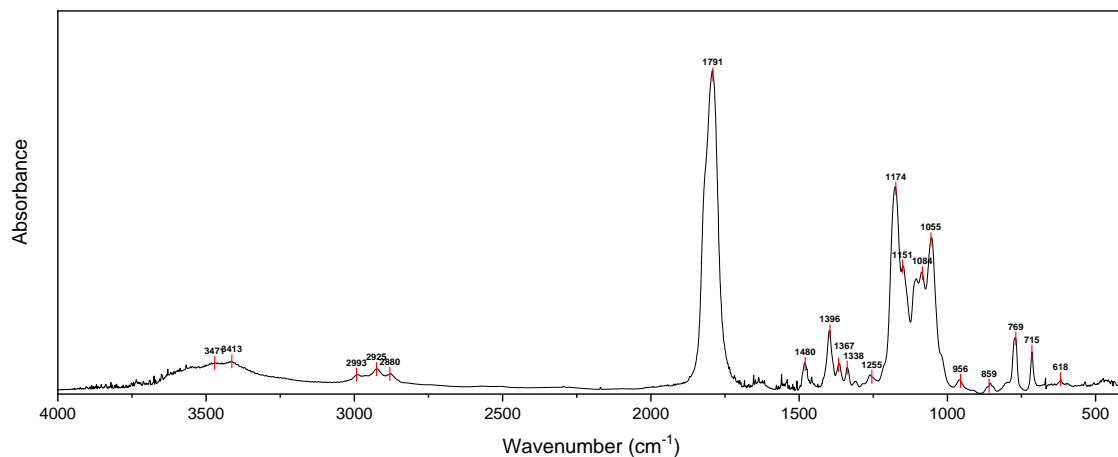


Figure 18: Top: FT-IR spectra of synthesized DGC, Down: FT-IR spectra of DGC from literature.

### 3.1.2 $^1\text{H}$ NMR analysis

According to Figure 19, the  $^1\text{H}$  NMR of our synthesized DGC is similar to that one of the literature, further indicating the successful synthesis of DGC.

For clarification, the peak at  $\sim 3.3\text{ppm}$  corresponds to the characteristic peak of the solvent (DMSO- $d_6$ ).

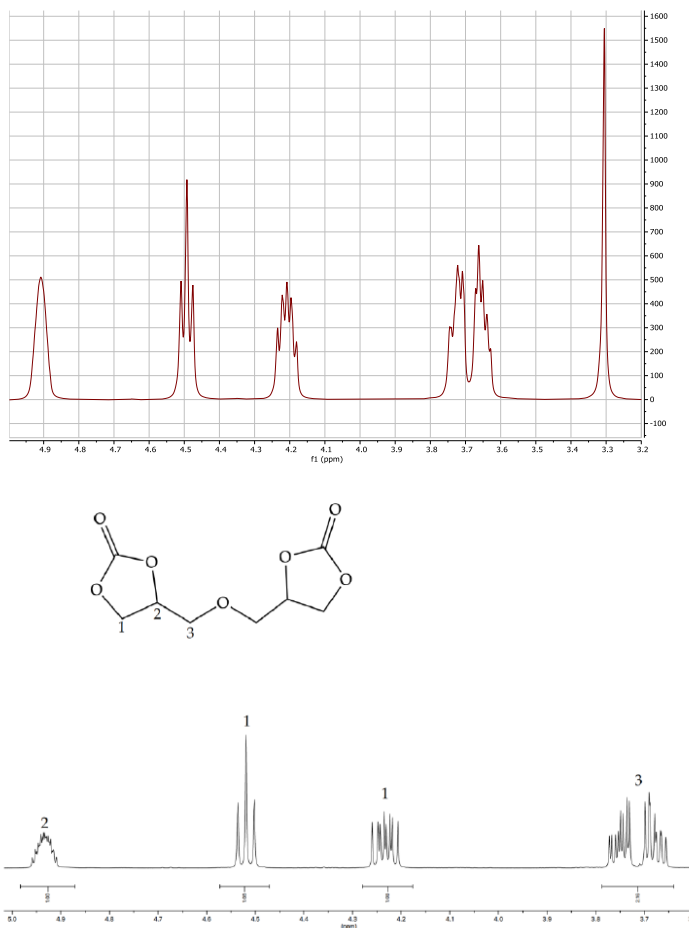


Figure 19:  $^1\text{H}$  NMR spectra of synthesized DGC, Down:  $^1\text{H}$  NMR spectra of DGC from literature.

### 3.1.3 TG analysis

Figure 20 presents the TG curve of the starting material, DIG. Based on these results, a maximum reaction temperature of 150 °C was selected to avoid degradation or decomposition phenomena observed at higher temperatures.

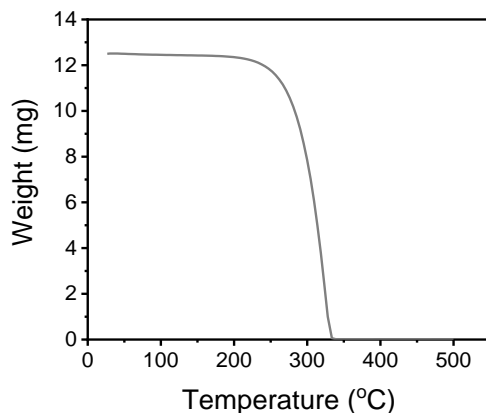


Figure 20: TG curve of DIG.

### 3.1.4 Dielectric properties

According to Figure 21, the studied system presents a polar–polar relationship between its product and reactant sides, and presents the microwave compatibility of all polar components (DIG, MeOH, DGC). It is noteworthy that the mixture’s polarity increases as the reaction progresses due to the transformation of the non-polar reactant (DMC) to the highly polar DGC and MeOH, making it more appropriate for MWH.

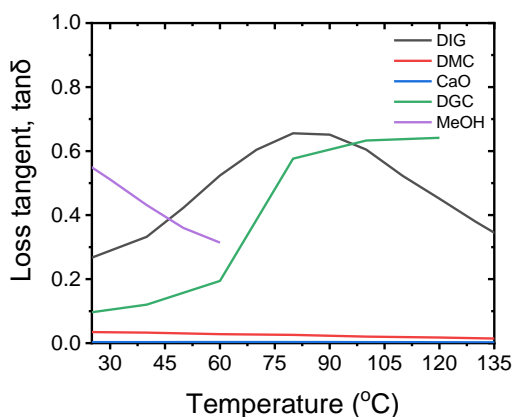


Figure 21: Loss tangent as a function of temperature/ dielectric properties

### 3.2 Effect of stirring

To initiate the evaluation of the reaction performance, an investigation was conducted to assess the potential influence of stirring speed on both the conversion of DIG and the yield of DGC. This initial analysis ensured that subsequent experiments could be conducted under optimized, yet simplified, stirring conditions without compromising reaction efficiency.

The experiments were conducted under identical conditions for both heterogeneous and homogeneous catalysis, changing only the stirring speed between 200 rpm and 400 rpm. For the heterogeneous system, CaO was used as the catalyst at 1% w/w<sub>DIG</sub>, with a DMC:DIG molar ratio of 6:1, at 130 °C for 2 hours. As shown in Figure 22, the conversion remained the same at 70% for both stirring speeds, as well as the yield, which remained close to 20%.

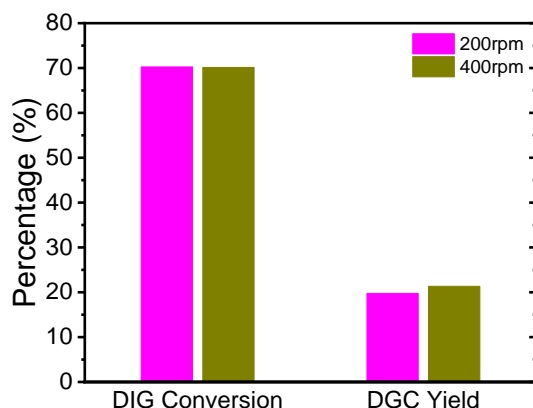


Figure 22: Effect of stirring on conversion and yield results/ heterogeneous catalyst

To verify whether this trend is similar in homogeneous systems as well, the experiments were carried out with NaOMe as the catalyst under the same temperature and molar ratio. As presented in Figure 23, the conversions and yields again remained constant, at about 90% and 55%, respectively.

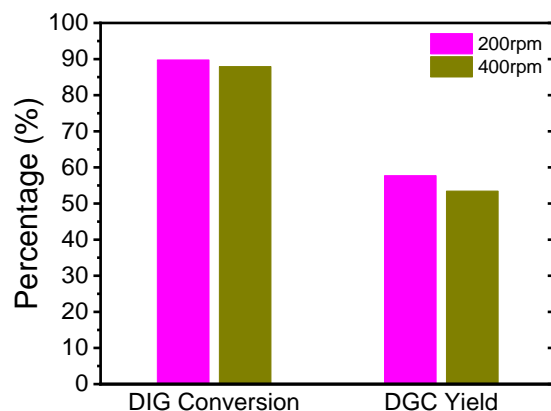


Figure 23: Effect of stirring on conversion and yield results/ homogeneous catalyst

These results demonstrate that, under the conditions tested, stirring speed does not influence either the conversion or yield, as no noticeable effects were observed. Based on this, the stirring speed of 200 rpm was selected for all subsequent experiments, as it ensures consistent mixing and higher speeds do not provide enhanced results.

### 3.3 Homogeneous vs heterogeneous catalysis

#### 3.3.1 Heterogeneous catalysis

The next part of this study is focused on evaluating the effect of each heating method, specifically comparing CH and MWH. Using the selected heterogeneous catalyst, CaO, a comparative study was conducted under identical reaction conditions for both modes. To be consistent, all experiments were carried out at 130 °C with a catalyst loading of 1% w/w<sub>DIG</sub> and a DMC:DIG molar ratio of 6:1, and the reaction time was adjusted at 2 hours.

The key indicators of the reaction progress, which are the conversion and yield obtained, are presented below in Figure 24 for both heating conditions. The results clearly show that MWH significantly outperformed CH, with the conversion increasing from 70% to 95% and the DGC yield improving from 19% to 61%.

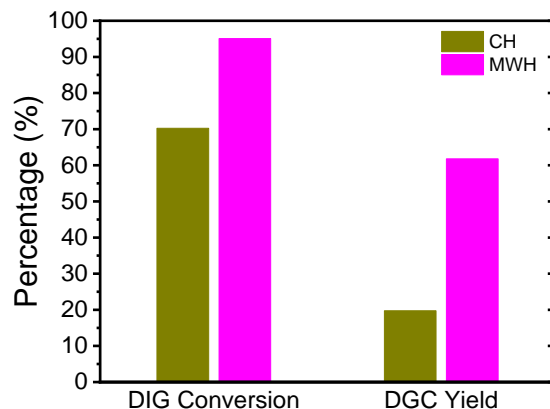


Figure 24: Comparison of DIG conversion (%) and DGC yield (%) under isothermal conditions for CH and MWH/ heterogeneous catalysis

For the same conditions, pressure was monitored in order to provide better understanding. The corresponding results are presented in Figure 25, which tracks the evolution of internal pressure over time for both heating methods. The pressure increase is notably faster and more pronounced under MWH, indicating a greater amount of MeOH in the vapor phase. Since MeOH is the main co-product of the transesterification reaction, this trend serves as a qualitative indicator of reaction progress. More specifically, the more rapid MeOH evolution under MWH suggests faster conversion of DIG and more efficient shifting of the reaction equilibrium toward DGC formation. The final pressure in the MWH at 4.6 bar is relatively higher than that of CH at 3.6 bar, supporting that better results were achieved.

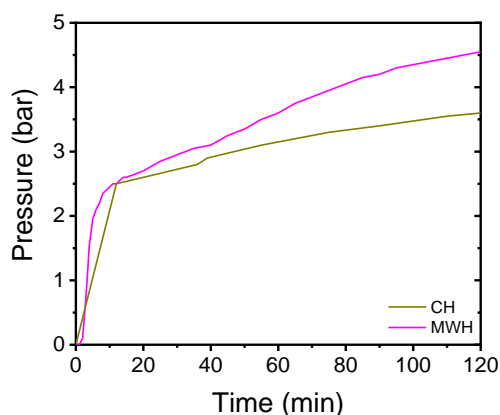


Figure 25: Evolution of pressure through reaction time for CH and MWH/ heterogeneous catalysis

Overall, these results confirm that MWH enhances the transesterification process when using CaO as a heterogeneous catalyst, offering significant improvements in both conversion and yield. The observed increase in pressure correlates with greater MeOH formation and leads to the conclusion that MWH accelerates reaction progress.

### 3.3.2 Homogeneous catalysis

Similarly to the previous part of the study, the effect of the heating method on reaction performance was investigated using NaOMe as a homogeneous catalyst. Experiments were conducted under the same conditions for both CH and MWH: 130 °C, 1% w/w<sub>DIG</sub> NaOMe, and a DMC:DIG molar ratio of 6:1, for 2 hours.

As shown in Figure 26, both CH and MWH result in nearly identical conversion and yield values when NaOMe is used as the catalyst. This could be due to the inherently higher catalytic strength of NaOMe, which already enables fast conversion under CH, potentially covering the additional benefits that MWH might otherwise provide. As presented by Ochoa-Gómez et al, although homogeneous catalysts exhibit higher catalytic activity than CaO and achieve greater conversions and yields under CH, their use introduces other challenges.<sup>18</sup> As a homogeneous catalyst, NaOMe requires more complex separation procedures and may contribute to higher operational costs and environmental concerns due to its solubility and potential toxicity.<sup>25</sup> For these reasons, while NaOMe is effective, it is not necessarily the optimal choice for sustainable process development.

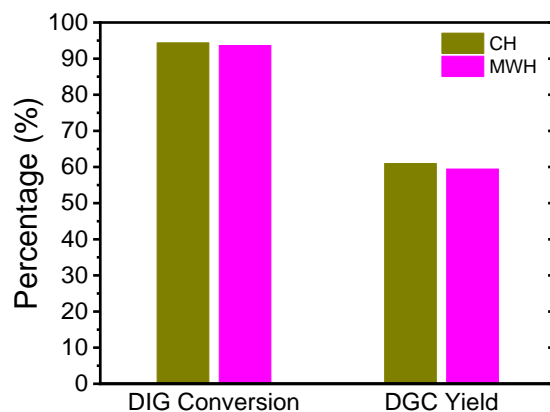


Figure 26: Comparison of DIG conversion (%) and DGC yield (%) under isothermal conditions for CH and MWH/heterogeneous catalysis

### 3.3.3 Comparison

The comparison between homogeneous and heterogeneous catalysis under different heating modes reveals that MWH significantly enhances the performance of CaO, allowing it to match the conversion and yield typically associated with NaOMe, as presented in Figure 27. This finding is particularly important as it demonstrates that a low-cost and environmentally friendly catalyst, such as CaO, can achieve comparable results when combined with the effects of MWH, that are to be discussed in the following section.

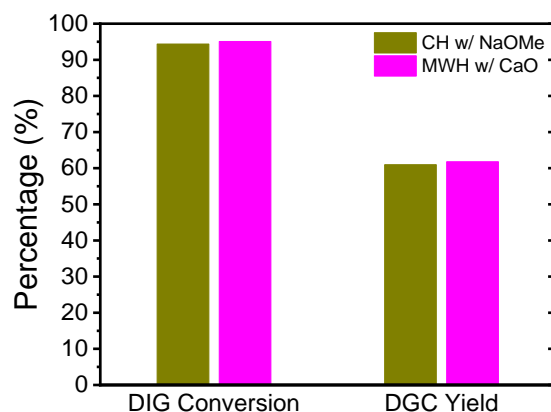


Figure 27: Comparison of conversion of DIG and yield of DGC for CH and MWH/ both types of catalyst

Overall, while NaOMe offers superior catalytic activity under CH conditions, it presents serious limitations in terms of sustainability and safety. It is highly corrosive and reacts violently with water, which is why it is typically employed as a 25–30% solution in MeOH in industrial processes.<sup>26</sup> Nevertheless, in the context of transesterification, where MeOH is a coproduct, its presence may adversely affect the reaction by shifting the equilibrium or altering catalyst activity. In contrast, CaO is inexpensive, non-toxic, and easily separated from the reaction mixture, making it a more attractive candidate for scalable and sustainable processes. Therefore, it will be further used to investigate the effects of MWH in the transesterification of DIG.

### 3.4 Isothermal operation

Based on the results of the previous section, it was concluded that the combination of MWH with a heterogeneous catalyst, and more specifically, CaO, offers a promising route for process intensification. Therefore, all the experiments were conducted using CaO, and as previously

mentioned, the three main parameters were investigated. Each parameter was varied to different values to assess its effect on conversion and yield, under both heating modes.

### 3.4.1 Catalyst loading

The first parameter to be examined was the role of catalyst loading on the performance of the reaction. For this part, a series of isothermal experiments were conducted varying CaO loading within the range of 0.1–2% w/w<sub>DIG</sub>. These experiments were carried out at a fixed DMC: DIG MR of 6:1, temperature of 130 °C, and reaction time of 2 hours.

The evolution of DIG conversion and DGC yield as a function of catalyst loading under both CH and MWH is displayed in Figure 28. It is shown that for MWH, increasing the CaO loading from 0.1% to 1.05% resulted in a substantial performance improvement, with conversion rising from 86% to 96% and yield increasing from 43% to 64%. In comparison, for CH, the conversion improved from 61% to 74%, and the DGC yield from 15% to 27%.

However, further increasing CaO loading from 1.05% to 2% under both modes does not improve results accordingly. To be precise, DGC yield increases by only 1–2% under both CH and MWH, while the conversion improvement under MWH is negligible. Lastly, CH shows a modest increase in conversion of approximately 5%. Overall, within the studied range, no CH condition achieved a combination of conversion and yield comparable to MWH, even at the highest catalyst loading of 2% w/w<sub>DIG</sub>.

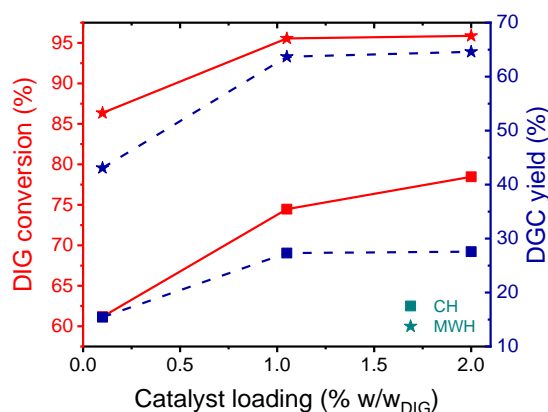


Figure 28: DIG conversion and DGC yield for experiments with DMC: DIG MR of 6:1, temperature of 130 °C, and reaction time of 2 hours.

The improved MWH results are also supported in Figure 29, which shows how the internal pressure within the reactor evolves with increasing catalyst loading. As mentioned, pressure serves as a qualitative indicator of reaction progress and is interconnected with the MeOH quantity in the vapor phase, meaning higher co-product concentrations increase the pressure. It is observed that under MWH, pressure increased more rapidly and reached higher values across all loadings, compared to CH.

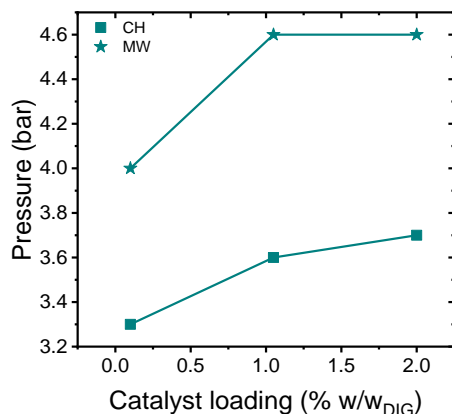


Figure 29: Autogenous pressure for experiments with DMC: DIG MR of 6:1, temperature of 130 °C, and reaction time of 2 hours.

The analytical results reveal that the catalyst loading of 2% leads to an increased accumulation of DGMC, the intermediate product. This observation suggests that the second step of the reaction, which is the conversion of DGMC to DGC, becomes limited under these conditions. As illustrated in Figure 30, the higher concentration of intermediate is accompanied by a decrease in the relative amount of MeOH present in the vapor phase. The insufficient removal of MeOH, combined with the increase of DGMC, translates to a lack of driving force under CH to shift the reaction from DGMC to DGC and reach the full progression of the reaction.

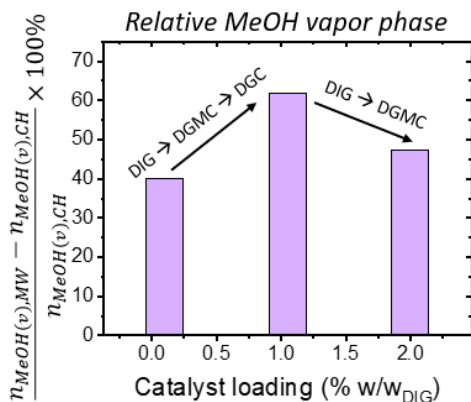


Figure 30: Relative MeOH vapor phase for experiments with DMC: DIG MR of 6:1, temperature of 130 °C, and reaction time of 2 hours.

This enhancement observed under MWH is attributed to the mixture's polarity and the presence of MeOH. The mixture's polarity increases as the reaction progresses due to the transformation of the non-polar reactant (DMC) to the highly polar DGC and MeOH. The rise in mixture's polarity translates into enhanced and continuously increased volumetric heat dissipation under MW irradiation. Combination of this effect with the presence of MeOH co-product, that has a significantly lower boiling point (65°C) compared to the other components, can intensify MeOH mass transfer from the liquid to the vapor phase under MWH and thereby enhance liquid phase reaction rates. This effect enhances the results in MWH as it shifts the equilibrium to the right and leads to higher conversion and yields.<sup>17</sup> Thus, the significance of the MWH effect is proven, particularly in combination with the low boiling point of MeOH.

### 3.4.2 DMC:DIG molar ratio

Following the next factor of optimization, the influence of the DMC:DIG MR on reaction performance was investigated under both CH and MWH. All experiments were conducted at 130 °C for 2 hours using 1.05% w/w<sub>DIG</sub> CaO as the catalyst. The goal was to determine how varying the amount of DMC affects conversion, yield, and the overall reaction environment.

As shown in Figure 31, increasing the MR from 2:1 to 6:1 led to a noticeable improvement in both DIG conversion and DGC yield. To be exact, during MWH mode conversion, the conversion rate rose from 78% to 96%, and the yield increased from 36% to 64%. Similarly, under CH, conversion increased from 67% to 74% and yield from 20% to 27%. These results suggest that a moderate excess of DMC is helpful and promotes the forward transesterification reaction.

Additionally, further increase in MR to 10:1 resulted in a decrease in both conversion and yield for both heating modes. This is attributed to two different factors: a decrease in effective catalyst concentration and a reduction in mixture polarity caused by the excess of non-polar DMC.

1. Usually, regarding transesterification reactions, an excessive DMC has a positive effect of shifting the reaction equilibrium to the right. Nevertheless, due to the increased volume, the excessive DMC also has a negative effect of limiting adequate contact between DIG and the catalyst. Finding the balance point between these two effects is an important concern in this process.<sup>27,28</sup>
2. The penetration depth of the microwaves into almost all nonpolar solvents is very deep when compared to polar solvents. As the mixture becomes less polar with excess DMC, its dielectric loss ( $\epsilon''$ ) and  $\tan \delta$  decrease, increasing microwave penetration depth and thus weakening the energy absorption essential for MWH effectiveness.<sup>29</sup>

That is why the effects mentioned are particularly evident under MWH, where, as mentioned, polar interactions are central to the heating mechanism.

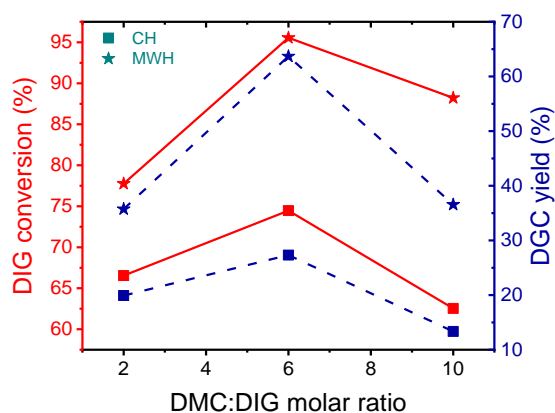


Figure 31: DIG conversion/DGC yield for experiments at 130 °C for 2 hours using 1.05% w/w<sub>DIG</sub> CaO

Overall, the results indicate that excessive use of DMC does not enhance reaction performance and may even hinder progress due to reduced catalytic effectiveness and less favorable solvent dynamics. Therefore, careful control of DMC:DIG MR is essential to ensure the balance between DMC excess and competing effects.

### 3.4.3 Temperature

Lastly, temperature was the final parameter evaluated under isothermal conditions, focusing again on understanding its influence on the reaction progression. All experiments for this section were conducted using CaO at 1.05% w/w<sub>DIG</sub>, a DMC: DIG MR of 6:1, and a reaction time of 2 hours.

The three temperature values for the experiments were 110, 130, and 150 °C. For the MWH mode, increasing the temperature from 110 °C to 130 °C led to an important improvement in performance, with conversion rising from 69% to 95% and DGC yield from 23% to 64%, as shown in Figure 32. Further augmentation to 150 °C offers slightly better results. Differently, under CH, a more gradual improvement was observed: increasing the temperature from 110 °C to 150 °C resulted in conversion rising from 38% to 96% and DGC yield from 6% to 65%. It is noteworthy that at the highest temperature, the gap between the conversions and yields of the two heating methods is insignificant. Attaining these results confirms that this parameter is the most influential in the transesterification of DIG when it comes to maximizing conversion and yield.

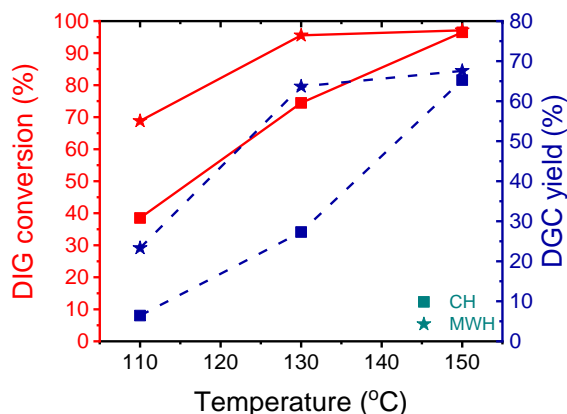


Figure 32: DIG conversion and DGC yield for experiments using CaO at 1.05% w/w<sub>DIG</sub>, DMC: DIG MR 6:1, and reaction time of 2 hours

Additionally, the relative quantity of MeOH in the vapor phase under MWH compared to CH, for the different temperatures, is illustrated in Figure 33. As expected, the highest difference between the two heating modes occurs at 130 °C, indicating that MWH facilitates faster and more effective MeOH removal at intermediate temperatures. However, at 150 °C, the difference diminishes, suggesting that the quantities of MeOH are similar, a fact that supports the closed levels of conversion and yield mentioned above.

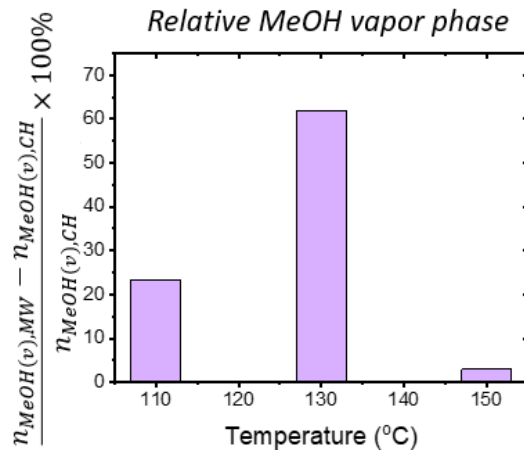


Figure 33: Relative MeOH vapor phase for experiments using CaO at 1.05% w/w<sub>DIG</sub>, DMC:DIG MR 6:1, and reaction time of 2 hours

Another factor that is under consideration is that at higher temperatures, the side reaction begins to have a great impact. Figure 34 shows that the yield of PG, the side product, increases steadily with temperature, regardless of the heating method. More specifically, above 130 °C, PG formation becomes significant, consuming valuable DIG and reducing selectivity toward DGC.<sup>15</sup>

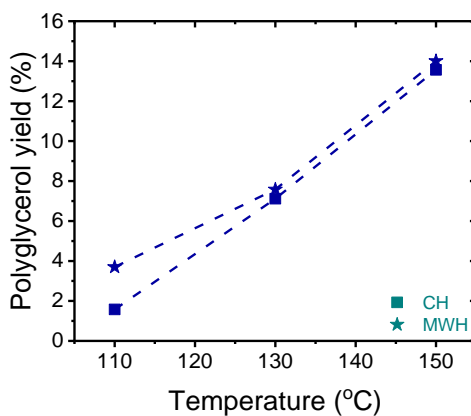


Figure 34: Polyglycerol yield for experiments using CaO at 1.05% w/w<sub>DIG</sub>, DMC:DIG MR 6:1, and reaction time of 2 hours

In summary, temperature was found to be the most influential factor affecting the transesterification reaction, significantly impacting DIG conversion and DGC yield through a dual effect based on Arrhenius-driven kinetics and enhanced MeOH vapor-phase transfer. Temperature raises the reaction progression rate by enhancing the rate, according to the Arrhenius principle. Simultaneously, temperature helps remove MeOH from the reaction mixture by turning it into vapor and shifting the equilibrium to the right, thus promoting higher product formation.

### 3.4.4 Overall comparison

To comprehensively assess the influence of the three examined parameters, response surface contour plots were constructed based on CCD using Response Surface Methodology (RSM). The display of the variation of DIG conversion for both heating modes is presented in Figure 35, while that of DGC yield is presented in Figure 36. The contour plots showcase the functions of catalyst loading and DMC:DIG molar ratio under the three distinct temperatures (110°C, 130°C, 150°C), offering a visual summary of the trends observed.

Among the three parameters investigated, temperature emerged as the most impactful. A rise from 110°C to 130°C produced a substantial increase in both DIG conversion and DGC yield across all cases, especially under MWH. At 150°C, nearly the entire area under both heating modes reached conversions above 90%, when the DGC yield correspondingly elevated at more than 60%. This underscores the importance of temperature in overcoming kinetic limitations (as described by the Arrhenius equation) and enhancing MeOH vaporization. While the temperature rises, the performance between CH and MWH becomes less pronounced, reflecting the temperature's ability to compensate for the absence of microwave-specific benefits on isothermal experiments.

Moving forward, the DMC:DIG molar ratio was the second most influential factor. Both DIG conversion and DGC yield increased with the molar ratio up to an optimum of approximately 6:1, beyond which a clear performance decline was observed. This is due to a drop in effective catalyst concentration caused by dilution when the DMC volume increases. Additionally, under MWH reduced polarity of the reaction medium caused by the excess non-polar DMC negatively affects microwave heat dissipation. These factors jointly reduce the driving force for the second transesterification step, resulting in lower attained yields.

In contrast, catalyst loading showcased the least sensitivity among the three variables, where increasing the catalyst from 0.1% to 2% w/w<sub>DIG</sub> resulted in only moderate gains. This trend is evident in each diagram along the catalyst axis, where conversions and yields are in the same range. This suggests that even though the presence of the catalyst is crucial, no substantial further rate enhancement occurs even with multiple quantities, especially at higher temperatures (>130°C).

Now, by comparing different triplets of the contour plots, it is confirmed that MWH consistently outperforms CH under most conditions, particularly at lower and intermediate temperatures ( $\leq 130^\circ\text{C}$ ). As already explained, the rise in mixture's polarity translates into enhanced and

continuously increased volumetric energy dissipation under MW irradiation. Combination of this effect with the presence of MeOH co-product that has a significantly lower boiling point (65°C) compared to the other components can intensify MeOH mass transfer from the liquid to the vapor phase under MWH and thereby enhance liquid phase reaction rates. The resulting shift in reaction equilibrium, based on Le Chatelier's principle, leads to better results.

In conclusion, temperature is the dominant factor governing reaction efficiency, followed by the DMC:DIG molar ratio, while catalyst loading plays a relatively minor role within the tested range. Therefore, to attain desirable results, temperature is maximized, the catalyst is minimized for reduced catalyst-related costs (purification, purchase, etc.), and the MR is adjusted to the optimal intermediate.

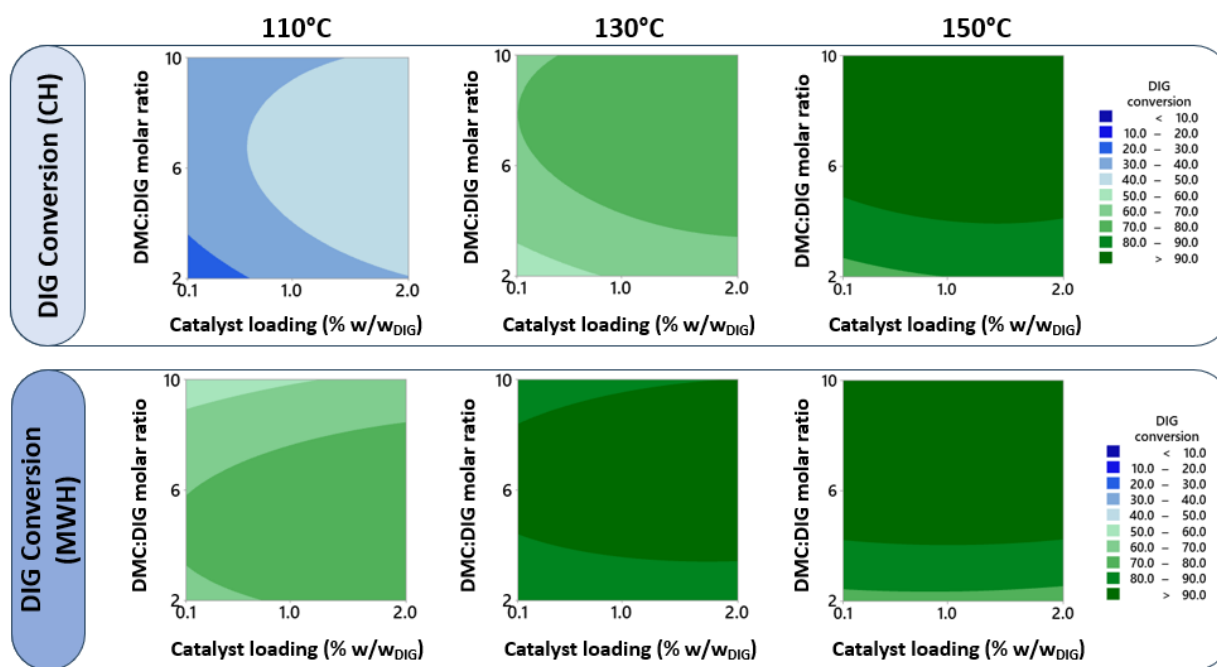


Figure 35: Overview of results for DIG conversion under CH and MWH

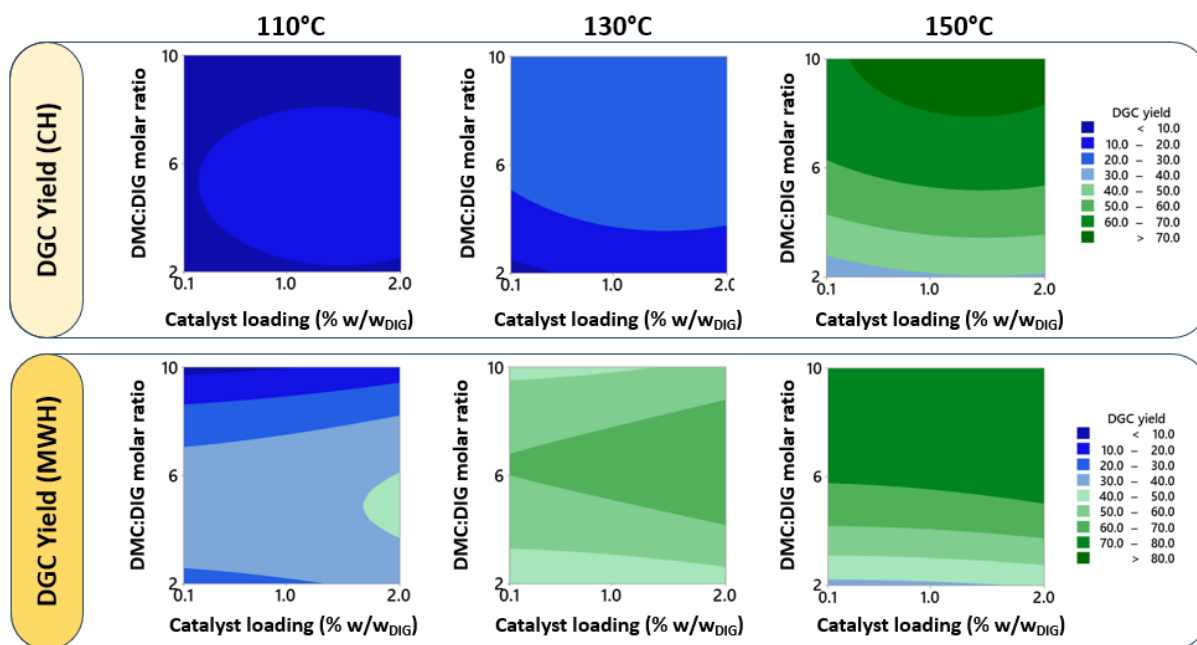


Figure 36: Overview of results for DGC yield under CH and MWH

### 3.5 Dynamic operation

Based on the isothermal operation screening, the optimal conditions that were used to further intensify the system are: reaction temperature at 150 °C, catalyst loading and DMC:DIG MR at 0.1% w/w<sub>DIG</sub> and 6:1, respectively.

According to the literature, it has been proven that the dynamic operation of MWs offers significant benefits compared to isothermal.<sup>17</sup>

Following the findings of Wang in the transesterification reaction of glycerol support that temperature cycling (TC) can improve the reaction progress as well as the energy consumption<sup>20</sup>. Therefore, TC was investigated at reaction conditions presented in Table 2, leading to six different cycling experiments carried out under microwave irradiation, alongside one reference experiment under isothermal CH.

This strategy aimed to further intensify the transesterification by achieving short-term exposure to elevated temperatures (> 150 °C), thereby enhancing the reaction kinetics while minimizing side reactions, such as DIG degradation and PG formation. As proven by the TGA analysis mentioned above, high temperatures are related to the degradation of the raw material, DIG. Each cycle consisted of heating to a target  $T_{max}$ , holding at that point for a defined period ( $T_{hold}$ ), followed by

a cooling phase to the minimum temperature  $T_{\min}$  and again holding it before repeating the cycle process three times. Temperatures and holding times differed in each experiment, as illustrated in Figure 37. Under these transient heating conditions, all temperature cycling profiles resulted in DIG conversions above 94% and DGC yields surpassing 54%, as shown in Table 3.

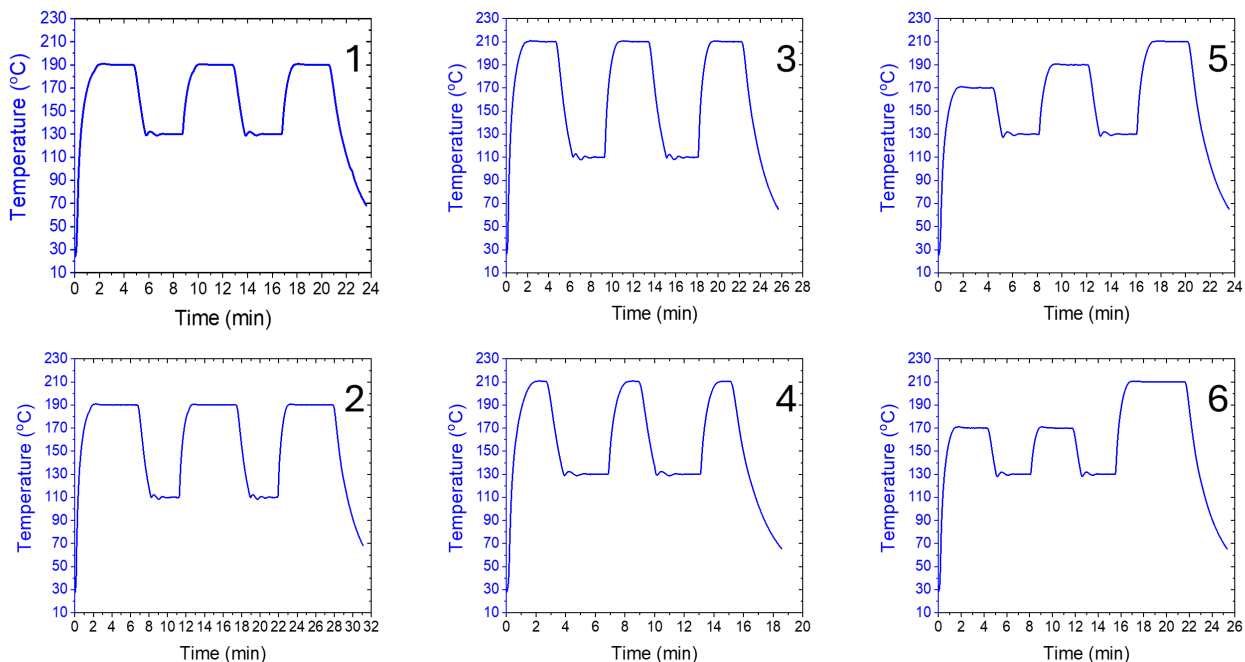


Figure 37: Temperature cycling profiles.

TC profile (#)	DIG conversion (%)	DGC yield (%)	DGMC yield (%)	Polyglycerol yield (%)
1	95	55	23	15
2	97	60	21	15
3	98	60	18	21
<b>4</b>	<b>98</b>	<b>73</b>	<b>17</b>	<b>7</b>
5	94	54	28	11
6	95	61	22	11
CH	93	59	19	15

Table 3: Results for temperature cycling experiments and CH experiments

It is observed that profiles with prolonged exposure to temperatures  $\geq 190$  °C for three minutes or more (e.g., cycles #1, #2, and #3) resulted in significantly increased polyglycerol formation. As already explained, extended high temperature holds favor the undesired self-condensation pathway over DGC route. Meanwhile, cycles #5 and #6, which applied a more gradual increase in  $T_{\max}$ , yielded higher DGMC and moderate DGC, when compared to cycle #4 (Table 3). Among all of the evaluated profiles, TC #4 achieved the best performance, providing a DGC yield of 73% while maintaining PG formation at just 7%, comparable to the levels typically observed at lower isothermal temperatures (e.g., 130 °C).

In addition to superior product yields, the use of TC significantly improved process efficiency. For the optimal TC, cycle #4, the transient profile reduced reaction time and energy demand ( $\text{kJ/mol}_{\text{DGC}}$ ) by 78% and 71%, respectively, when compared to CH isothermal operation. These findings confirm that the dynamic operation of MWH through TC not only enhances conversion and yield but also minimizes side product formation and reduces the overall energy footprint of the process. This aligns with the green chemistry goals of the NIPU production.

## Conclusions

This study provides insights for the first time on the transesterification of DIG with DMC to produce DGC and MeOH under CH and MWH in batch systems operating at autogenous pressure. Unlike previous studies that typically employ CH in reflux conditions, this work explores MWH-assisted operation as an alternative heating approach. The main goal is to exceed conversions and yields while minimizing energy requirements compared to conventionally heated systems, with the use of a heterogeneous catalyst.

DGC was successfully synthesized through a batch transesterification 2-step process, which includes the reaction of DIG with DMC to form an intermediate (DGMC) (step 1) that further reacts with DMC to synthesize the final product, DGC (step 2). The study investigates DIG transesterification under two distinct operating regimes: 1) Isothermal operation, where the effects of key reaction parameters, including catalyst loading, DMC:DIG molar ratio, and temperature are systematically evaluated; and 2) Dynamic operation under MWH, in which temperature cycling is applied to potentially further enhance reaction performance.

The samples produced from the experiments were analyzed with FT-IR, NMR, TG, and most importantly, HPLC to assess qualitative as well as quantitative results. The conversion of DIG, the DGC yield, and the energy consumption were calculated and were set as the main criteria to evaluate each of the key parameters.

Therefore, crucial conclusions were reached:

1. The experimental procedure consistently yielded DGC under both CH and MWH modes. This was confirmed by FT-IR, NMR, and TG analysis and their comparison to literature findings.
2. Preliminary analysis showed that stirring speed does not influence the conversion of DIG or the yield of DGC under the conditions tested. This was consistent across both catalyst types and heating methods, and a stirring speed of 200 rpm was chosen for all subsequent experiments to ensure consistency.
3. When comparing homogeneous and heterogeneous catalysis, it was found that MWH significantly boosts the performance of heterogeneous (CaO) systems, allowing them to match conversion and yield values typically attained in homogeneous catalysis (NaOMe). This is

particularly important since CaO is a low-cost, environmentally friendly catalyst, and when paired with MWH, it becomes an ideal candidate for this transesterification process.

4. In order to investigate the impact of catalyst loading, DMC:DIG molar ratio, and temperature, a CCD was employed. Contour plots were generated to visualize the performance trends under both heating modes and to highlight interactions among the three variables.
5. Temperature emerged as the most impactful variable. Increasing the reaction temperature from 110°C to 130°C resulted in substantial increases in both DIG conversion and DGC yield, especially under MWH. At 150°C, both heating methods' conversion levels surpassed 90% and DGC yields reached over 60% across catalyst loading and DMC:DIG MR range tested, resulting in similar values for both modes. This demonstrates that elevated temperatures enhance reaction progression, based on Arrhenius law, while also increasing MeOH vaporization. These two factors synergistically shift the equilibrium toward product formation, while the temperature increase is mitigated by higher production rates of side product, PG.
6. The DMC: DIG molar ratio was the second most influential parameter. Raising the ratio from 2:1 to 6:1 improved both conversion and yield, but further increases led to moderate performance. This is due to a drop in effective catalyst concentration caused by dilution when DMC volume increases. Additionally, under MWH reduced polarity of the reaction medium caused by the excess non-polar DMC negatively affects microwave heat dissipation.
7. Catalyst loading had the least impact within the tested range (0.1–2% w/w<sub>DIG</sub>). While increasing the catalyst amount improved conversion and yield slightly, the gains were minimal and diminished at higher temperatures. This suggests that even though catalyst presence is essential, once a certain level of catalytic activity is achieved, further addition does not influence the results.
8. MWH outperformed CH in most scenarios, particularly at lower to intermediate temperatures. The higher polarity of the reaction mixture under MWH, combined with the low boiling point of MeOH, enhances heat dissipation and facilitates the vapor-phase transfer of MeOH. This leads to an effective shift in reaction equilibrium, as stated by Le Chatelier's principle.
9. The relative importance of each parameter was established as follows: temperature > DMC:DIG molar ratio > catalyst loading. To achieve optimal conditions, the temperature should be elevated, the catalyst amount minimized to reduce cost and complexity, and the molar ratio maintained around 6:1 to balance reactant excess and catalytic effectiveness.

10. To further intensify the process, dynamic MWH using temperature cycling was evaluated. Among six profiles tested, the profile consisting of short high-temperature  $T_{\max}$  but for relatively short  $T_{\text{hold}}$  delivered the best performance: 98% DIG conversion, 73% DGC yield, only 7% polyglycerol by-product, and significantly improved selectivity.
11. The same experiment also achieved outstanding process efficiency, reducing reaction time and energy demand by 78% and 71%, respectively, compared to CH under isothermal conditions. This improvement in energy efficiency, combined with enhanced reactant conversion and product yield, renders MWH transient profiles as a promising alternative energy source for intensified DGC production.

It is finally remarked that the findings presented in this work are directly relevant to a broad class of equilibrium liquid phase reactions entailing low-boiling point products present in polar reactive systems with reactants of higher boiling point. Batch processes involving such chemistries can be intensified by the application of MWH due to efficient heat dissipation.

The concept leverages the mixture polarity to enable rapid volumetric energy transfer that enhances the removal of the most volatile product compound(s) and drives the reaction toward equilibrium states corresponding to higher reactant conversion levels that are unattainable by CH.

## References

- (1) Turnaturi, R.; Zagni, C.; Patamia, V.; Barbera, V.; Floresta, G.; Rescifina, A. CO<sub>2</sub>-Derived Non-Isocyanate Polyurethanes (NIPUs) and Their Potential Applications. *Green Chemistry* **2023**, pp 9574–9602. <https://doi.org/10.1039/d3gc02796a>.
- (2) Sathiyavimal, S.; Vasantharaj, S.; LewisOscar, F.; Selvaraj, R.; Brindhadevi, K.; Pugazhendhi, A. Natural Organic and Inorganic–Hydroxyapatite Biopolymer Composite for Biomedical Applications. *Progress in Organic Coatings*. **2020** <https://doi.org/10.1016/j.porgcoat.2020.105858>.
- (3) Sonnenschein, M. F. *Polyurethanes: Science, Technology, Markets, and Trends*; John Wiley & Sons, Inc.: Hoboken, NJ, **2015**. <https://doi.org/10.1002/9781118901274>.
- (4) Maisonneuve, L.; Lamarzelle, O.; Rix, E.; Grau, E.; Cramail, H. Isocyanate-Free Routes to Polyurethanes and Poly(Hydroxy Urethane)s. *Chemical Reviews* **2015**, pp 12407–12439. <https://doi.org/10.1021/acs.chemrev.5b00355>.
- (5) Mundo, F.; Caillol, S.; Ladmiraal, V.; Meier, M. A. R. On Sustainability Aspects of the Synthesis of Five-Membered Cyclic Carbonates. *ACS Sustainable Chemistry and Engineering* **2024**, pp 6452–6466. <https://doi.org/10.1021/acssuschemeng.4c01274>.
- (6) Balla, E.; Bikiaris, D. N.; Pardalis, N.; Bikiaris, N. D. Toward Sustainable Polyurethane Alternatives: A Review of the Synthesis, Applications, and Lifecycle of Non-Isocyanate Polyurethanes (NIPUs). *Polymers (Basel)* **2025**, *17* (10), 1364. <https://doi.org/10.3390/polym17101364>.
- (7) Cornille, A.; Auvergne, R.; Figovsky, O.; Boutevin, B.; Caillol, S. A Perspective Approach to Sustainable Routes for Non-Isocyanate Polyurethanes. *European Polymer Journal* **2017**, pp 535–552. <https://doi.org/10.1016/j.eurpolymj.2016.11.027>.
- (8) Theerathanagorn, T.; Kessaratikoon, T.; Rehman, H. U.; D’Elia, V.; Crespy, D. Polyhydroxyurethanes from Biobased Monomers and CO<sub>2</sub>: A Bridge between Sustainable Chemistry and CO<sub>2</sub> Utilization†. *Chinese Journal of Chemistry* **2024**, pp 652–685. <https://doi.org/10.1002/cjoc.202300531>.
- (9) Tryznowski, M.; Świdarska, A. Novel High Reactive Bifunctional Five-And Six-Membered Bicyclic Dicarboxylate-Synthesis and Characterisation. *RSC Adv* **2018**, *8* (21), 11749–11753. <https://doi.org/10.1039/c8ra00669e>.
- (10) Tryznowski, M.; Świdarska, A.; Zołek-Tryznowska, Z.; Gołofit, T.; Parzuchowski, P. G. Facile Route to Multigram Synthesis of Environmentally Friendly Non-Isocyanate Polyurethanes. *Polymer (Guildf)* **2015**, *80*, 228–236. <https://doi.org/10.1016/j.polymer.2015.10.055>.

- (11) Van Velthoven, J. L. J.; Gootjes, L.; Van Es, D. S.; Noordover, B. A. J.; Meuldijk, J. Poly(Hydroxy Urethane)s Based on Renewable Diglycerol Dicarboxylate. *Eur Polym J* **2015**, *70*, 125–135. <https://doi.org/10.1016/j.eurpolymj.2015.07.011>.
- (12) Younes, G. R.; Price, G.; Dandurand, Y.; Maric, M. Study of Moisture-Curable Hybrid NIPUs Based on Glycerol with Various Diamines: Emergent Advantages of PDMS Diamines. *ACS Omega* **2020**, *5* (47), 30657–30670. <https://doi.org/10.1021/acsomega.0c04689>.
- (13) Stewart, J. A.; Drexel, R.; Arstad, B.; Reubsæet, E.; Weckhuysen, B. M.; Bruijninx, P. C. A. Homogeneous and Heterogenised Masked N-Heterocyclic Carbenes for Bio-Based Cyclic Carbonate Synthesis. *Green Chemistry* **2016**, *18* (6), 1605–1618. <https://doi.org/10.1039/c5gc02046h>.
- (14) Aresta, M.; Dibenedetto, A.; Di Bitonto, L. New Efficient and Recyclable Catalysts for the Synthesis of Di- and Tri-Glycerol Carbonates. *RSC Adv* **2015**, *5* (79), 64433–64443. <https://doi.org/10.1039/c5ra06981e>.
- (15) Stewart, J. A.; Weckhuysen, B. M.; Bruijninx, P. C. A. Reusable Mg-Al Hydrotalcites for the Catalytic Synthesis of Diglycerol Dicarboxylate from Diglycerol and Dimethyl Carbonate. *Catal Today* **2015**, *257* (Part 2), 274–280. <https://doi.org/10.1016/j.cattod.2014.06.035>.
- (16) Ardila-Suárez, C.; Rojas-Avellaneda, D.; Ramirez-Caballero, G. E. Effect of Temperature and Catalyst Concentration on Polyglycerol during Synthesis. *Int J Polym Sci* **2015**, *2015*. <https://doi.org/10.1155/2015/910249>.
- (17) Papaioannou, I.; Arampatzis, A.; Tzortzi, I.; Gao, X.; Van Gerven, T.; Stefanidis, G. D. Intensification of Ethylene Carbonate Synthesis via Microwave-Induced Phase-Change Cycles. *ChemSusChem* **2025**. <https://doi.org/10.1002/cssc.202500099>.
- (18) Ochoa-Gómez, J. R.; Gómez-Jiménez-Aberasturi, O.; Maestro-Madurga, B.; Pesquera-Rodríguez, A.; Ramírez-López, C.; Lorenzo-Ibarreta, L.; Torrecilla-Soria, J.; Villarán-Velasco, M. C. Synthesis of Glycerol Carbonate from Glycerol and Dimethyl Carbonate by Transesterification: Catalyst Screening and Reaction Optimization. *Appl Catal A Gen* **2009**, *366* (2), 315–324. <https://doi.org/10.1016/j.apcata.2009.07.020>.
- (19) Farias da Costa, A. A.; de Nazaré de Oliveira, A.; Esposito, R.; Auvigne, A.; Len, C.; Luque, R.; Rodrigues Noronha, R. C.; Santos do Nascimento, L. A. Glycerol and Microwave-Assisted Catalysis: Recent Progress in Batch and Flow Devices. *Sustainable Energy and Fuels*. Royal Society of Chemistry March 10, **2023**, pp 1768–1792. <https://doi.org/10.1039/d2se01647h>.
- (20) Wang, S.; Xu, L.; Okoye, P. U.; Li, S.; Tian, C. Microwave-Assisted Transesterification of Glycerol with Dimethyl Carbonate over Sodium Silicate Catalyst in the Sealed Reaction

- System. *Energy Convers Manag* **2018**, *164*, 543–551.  
<https://doi.org/10.1016/j.enconman.2018.03.021>.
- (21) Rzepecka, M. A. A Cavity Perturbation Method for Routine Permittivity Measurement\*. *J. Microw. Power* **1973**, *8* (1), 3–11. <https://doi.org/10.1080/00222739.1973.11689015>.
- (22) Van Velthoven, J. L. J.; Gootjes, L.; Van Es, D. S.; Noordover, B. A. J.; Meuldijk, J. Poly(Hydroxy Urethane)s Based on Renewable Diglycerol Dicarboxylate. *Eur Polym J* **2015**, *70*, 125–135. <https://doi.org/10.1016/j.eurpolymj.2015.07.011>.
- (23) Calvino-Casilda, V.; Mul, G.; Fernández, J. F.; Rubio-Marcos, F.; Bañares, M. A. Monitoring the Catalytic Synthesis of Glycerol Carbonate by Real-Time Attenuated Total Reflection FTIR Spectroscopy. *Appl Catal A Gen* **2011**, *409–410*, 106–112. <https://doi.org/10.1016/j.apcata.2011.09.036>.
- (24) Aresta, M.; Dibenedetto, A.; Di Bitonto, L. New Efficient and Recyclable Catalysts for the Synthesis of Di- and Tri-Glycerol Carbonates. *RSC Adv* **2015**, *5* (79), 64433–64443. <https://doi.org/10.1039/c5ra06981e>.
- (25) Thangaraj, B.; Solomon, P. R.; Muniyandi, B.; Ranganathan, S.; Lin, L. Catalysis in Biodiesel Production - A Review. *Clean Energy*. Oxford University Press February 27, **2019**, pp 2–23. <https://doi.org/10.1093/ce/zky020>.
- (26) Alptekin, E.; Canakci, M. Optimization of Transesterification for Methyl Ester Production from Chicken Fat. *Fuel* **2011**, *90* (8), 2630–2638. <https://doi.org/10.1016/j.fuel.2011.03.042>.
- (27) Wang, S.; Wang, J.; Sun, P.; Xu, L.; Okoye, P. U.; Li, S.; Zhang, L.; Guo, A.; Zhang, J.; Zhang, A. Disposable Baby Diapers Waste Derived Catalyst for Synthesizing Glycerol Carbonate by the Transesterification of Glycerol with Dimethyl Carbonate. *J Clean Prod* **2019**, *211*, 330–341. <https://doi.org/10.1016/j.jclepro.2018.11.196>.
- (28) Ochoa-Gómez, J. R.; Gómez-Jiménez-Aberasturi, O.; Maestro-Madurga, B.; Pesquera-Rodríguez, A.; Ramírez-López, C.; Lorenzo-Ibarreta, L.; Torrecilla-Soria, J.; Villarán-Velasco, M. C. Synthesis of Glycerol Carbonate from Glycerol and Dimethyl Carbonate by Transesterification: Catalyst Screening and Reaction Optimization. *Appl Catal A Gen* **2009**, *366* (2), 315–324. <https://doi.org/10.1016/j.apcata.2009.07.020>.
- (29) Palma, V.; Barba, D.; Cortese, M.; Martino, M.; Renda, S.; Meloni, E. Microwaves and Heterogeneous Catalysis: A Review on Selected Catalytic Processes. *Catalysts*. MDPI February 1, **2020**. <https://doi.org/10.3390/catal10020246>.

## Acknowledgements

This thesis is the result of a collective effort involving the valuable support of several individuals. First and foremost, I would like to sincerely thank PhD candidate John Papaioannou for his guidance, supervision, and review of my work, as well as for his constant availability to discuss theoretical issues and assist throughout the experimental process. I am also grateful to the other members of the Laboratory of Chemical Process Engineering, Thanasis Arampatzis and Katerina Zerva, for their willingness to offer support whenever questions or difficulties arose, and for their presence, which contributed greatly to a positive and supportive laboratory environment.

I would also like to express my appreciation to my supervising professor, George Stefanidis, whose scientific guidance and collaboration were essential for the successful completion of this thesis.

Finally, I dedicate this work to my family and friends. Their encouragement and support have been a vital source of strength, not only for the completion of this thesis but throughout my academic journey.

Η εκπόνηση αυτής της εργασίας είναι αποτέλεσμα συλλογικής προσπάθειας και υποστήριξης από πολλούς ανθρώπους. Πρώτα απ' όλα, θα ήθελα να ευχαριστήσω θερμά τον υποψήφιο διδάκτορα Γιάννη Παπαϊωάννου για την καθοδήγηση, την επίβλεψη και τον έλεγχο της πορείας της εργασίας μου, καθώς και για τη σταθερή του διαθεσιμότητα να συζητήσει θεωρητικά ζητήματα και να συνδράμει στη διεξαγωγή των πειραμάτων. Επίσης, ευχαριστώ τα υπόλοιπα μέλη του Εργαστηρίου Τεχνικής Χημικών Διεργασιών, τον Θανάση Αραμπατζή και την Κατερίνα Ζέρβα, για την προθυμία τους να βοηθήσουν σε κάθε απορία ή ανάγκη που προέκυψε κατά την πειραματική διαδικασία, αλλά και για τη φιλική τους παρουσία, που αποτέλεσε πολύτιμη στήριξη κατά την παραμονή μου στο εργαστήριο.

Θα ήθελα, ακόμη, να εκφράσω την ευχαριστία μου στον επιβλέποντα καθηγητή μου, Γεώργιο Στεφανίδη, του οποίου η επιστημονική καθοδήγηση και συνεργασία υπήρξαν καθοριστικές για την υλοποίηση αυτής της διπλωματικής εργασίας.

Τέλος, η εργασία αυτή αφιερώνεται στην οικογένειά μου και στους φίλους μου, των οποίων η στήριξη υπήρξε σημαντική όχι μόνο για την ολοκλήρωση του παρόντος έργου, αλλά και συνολικά για την ακαδημαϊκή μου πορεία.

## List of Abbreviations

<b>Abbreviation</b>	<b>Full Term</b>
<b>BCCs</b>	Bis-cyclic carbonates
<b>CCD</b>	Central Composite Design
<b>CH</b>	Conventional Heating
<b>DGC</b>	Diglycerol Dicarboxylate
<b>DGMC</b>	Diglycerol Monocarbonate
<b>DIG</b>	Diglycerol
<b>DMC</b>	Dimethyl Carbonate
<b>MCCs</b>	Mono-cyclic carbonates
<b>MeOH</b>	Methanol
<b>MR</b>	Molar Ratio
<b>MWH</b>	Microwave Heating
<b>NIPUs</b>	Non-Isocyanate Polyurethanes
<b>PG</b>	Polyglycerol
<b>PHUs</b>	Polyhydroxyurethanes
<b>PUs</b>	Polyurethanes